MATHEMATICAL MODELING AND TESTING OF A NEW POLYMER-BASED IMPACT TOOL DESIGN TO REDUCE VIBRATION-RELATED BIOMECHANICAL INJURIES

by

Janelle A. Konchar

A thesis submitted to the Faculty of the University of Delaware in partial fulfillment of the requirements for the Degree of Bachelor of Mechanical Engineering with Distinction.

Spring 2006

MATHEMATICAL MODELING AND TESTING OF A NEW POLYMER-BASED IMPACT TOOL DESIGN TO REDUCE VIBRATION-RELATED BIOMECHANICAL INJURIES

by

Janelle A. Konchar

Approved: _____
Dr. James L. Glancey, Ph.D.
Professor in charge of thesis on behalf of the Advisory Committee

Approved: _____
Dr. John Novotny, Ph.D.
Committee member from the Department of Mechanical Engineering

Approved: _____
Dr. John Pelesko, Ph.D.
Committee member from the Board of Senior Thesis Readers

Approved: _____
Mohsen Badiey, Ph.D.
Chair of the University Committee on Student and Faculty Honors

ACKNOWLEDGMENTS

TABLE OF CONTENTS

Chapter

LIST OF TABLES

LIST OF FIGURES

ABSTRACT

Power tools continue to be a source of high vibration in the workplace with long-term affects on the user contributing to many biomechanical ailments including Hand-Arm Vibration Syndrome (HAV), Raynaud's phenomenon, and white finger. Tools with reciprocating impact components typically produce accelerations that induce vibration-related injuries unless the daily exposure and/or dosage is limited. To examine the potential for reducing vibrations emitted from power impact tools, a model of the impact mechanism has been developed. The first order differential equations describing the motion of the piston-tool system were simulated in Matlab, and alternate system designs were evaluated. A modified cutting chisel that included a high-performance engineering polymer insert was examined. Experiments with a prototype chisel and insert revealed that acceleration magnitudes in the axial (cutting) direction were reduced. Simulations and laboratory testing also investigated chisel force transmission characteristics. While a chisel with a polymer insert slightly reduced maximum chisel output forces, the reduction was found to be statistically insignificant (at the 95% confidence level). High frequency testing using an Instron™ material test machine replicated force transmission and demonstrated polymer degradation as a function of the number of loading cycles. Future work is recommended on selecting a polymer material and geometry suitable to meet the life-load requirements.

Keywords: power tool, impact, vibration, biomechanical injury, safety, ergonomics, engineering polymers

Chapter 1

INTRODUCTION

1.1   Background

Power tools have a large market presence and are valued as important pieces of equipment in industries worldwide. Traditional power tools with reciprocating impact components produce vibration energy that is transmitted to the tool user. Exposure to vibrations emitted from power impact tools represents a significant workplace hazard contributing to serious worker health problems and biomechanical injuries such as Raynaud's phenomenon, Hand-Arm Vibration Syndrome (HAVS), and white finger. Recent data specifies that injuries associated with hand tool operation comprised 5.2% (65,450) of the total work-related injury cases in the United States [1]. Out of these cases, 26.6% (17,390) involved injury resulting specifically from power hand tools [1]. Hand Arm Vibration (HAV) alone affects two million U.S. workers [2].

The use of tools expose users (workers) to high levels of vibration that can cause permanent, irreversible damage to blood vessels and nerves in the hand and arm. Often, hand-arm injuries are accompanied by hearing loss attributed to exposure to high vibration (and sound). In 2001, the U.S Department of Labor's Occupational Safety and Health Administration (OSHA) published ergonomics rules for all general industry employers [3]. Within this Standard, vibration and the use of hand tools was identified as one of five ergonomic risks factors leading to injury or symptoms for work-related musculoskeletal disorders.

Excessive HAV exposure from vibrating pneumatic, electric, hydraulic, or gasoline-powered hand tools can produce an irreversible damage to the hands [2]. As a result of the increasing ergonomic awareness and employer concern surrounding occupational vibration injury caused by the regular use of tools in the workplace, this study has been initiated to develop a new impact tool design to reduce vibration-related biomechanical injuries. Proof of concept and evaluation of this new design will be accomplished using a pneumatic-powered hand tool.

1.2   Objectives of this Study

The overall goal of this work is to improve conventional power tool design using high-performance engineering polymers in order to reduce the harmful biomechanical ailments associated with their long-term use. Previous work has reported a methodology for evaluating and modifying the vibration characteristics of power tools for the characterization of commercially available low-vibration power tools [4].

For the purpose of this study, work will focus on hand-held power tools with an emphasis on the design and performance of pneumatic-powered reciprocating tools. The specific objectives are to model the tool system impact mechanism, prototype new tool components, and evaluate through modeling and testing possible improvements gained from integrating engineering polymers into traditional power tool designs.

Chapter 2

CONCEPTUAL DEVELOPMENT

2.1   Mechanics of the Pneumatic Impact Tool

A simple schematic of a pneumatic tool system is shown in Figure 1. Pneumatic

tools are powered by compressed air. A Dayton Model ZZ486C, shown in Figure 2, is a

conventional power chisel. When the trigger is pulled a valve in the tool chamber opens,

allowing air pressure to be applied to the back of the piston. During the stroke of the

piston, the relative location of air passages with respect to piston position changes,

causing the oscillatory nature of the piston motion. Placement of these air passages

allows air to flow in one direction during the piston down stroke, and air to flow in the

opposite direction during piston reversal. As the piston reaches maximum allowable

stroke length within the tool cylinder, impact occurs between the piston front and the top

end of the chisel, extending the chisel for cutting into the desired "work". A safety

retainer keeps the chisel seated against the chamber and prevents the chisel accessory

from ejection during tool operation.
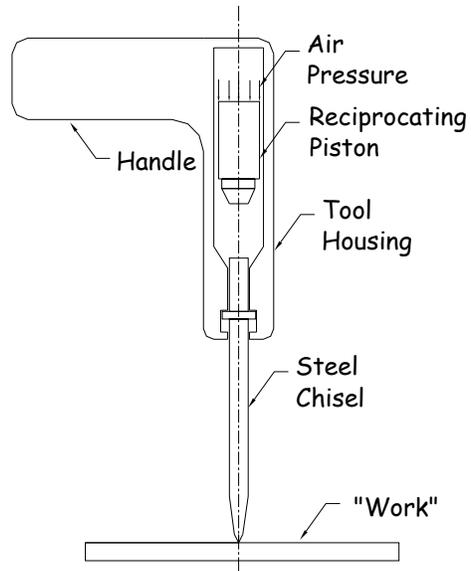
Figure 1.   Conceptual View of a Pneumatic Chisel.

Figure 2.   Photograph of the Dayton Model ZZ486C instrumented pneumatic chisel used for experimental testing.

2.2   Design Considerations for Low Vibration and Sound

The impact between the steel piston and steel chisel is the principle sources of vibration generated by the tool system. By integrating advanced engineering polymers into current power tool designs, the direct metal-to-metal contact between the piston and chisel components can be eliminated. The ambition of this material substitution, to dissipate the overall vibration magnitude and remove harmful frequencies of vibration transmitted to the hand and arm extremities, represents a significant improvement in the safety of conventional tool systems. Furthermore, this ergonomic performance enhancement must be achieved without compromising the cutting performance of the power tool.

2.3   Preliminary Prototypes and Proof of Concept

Early demonstration of the potential advantages of integrating polymers into power tool design was achieved through modification of the piston component. Duplicate pistons were reliably fabricated at low cost using a standard lathe. Replicate steel pistons were adapted into two prototype treatments, one incorporating polymer material at the front impact end of the piston while the second concept added polymer material to the back surface of the piston (see Figure 3). To accommodate a front insert, a hole was drilled into the piston allowing a cylindrical polymer insert to be pressed (interference fit) into the cavity created from the removed steel material. The back insert configuration required no additional machining to the duplicate piston; a 3 mm thick circular polymer disk of equal diameter to the rear piston face was secured to the piston back using a high-performance, two-part epoxy.

14
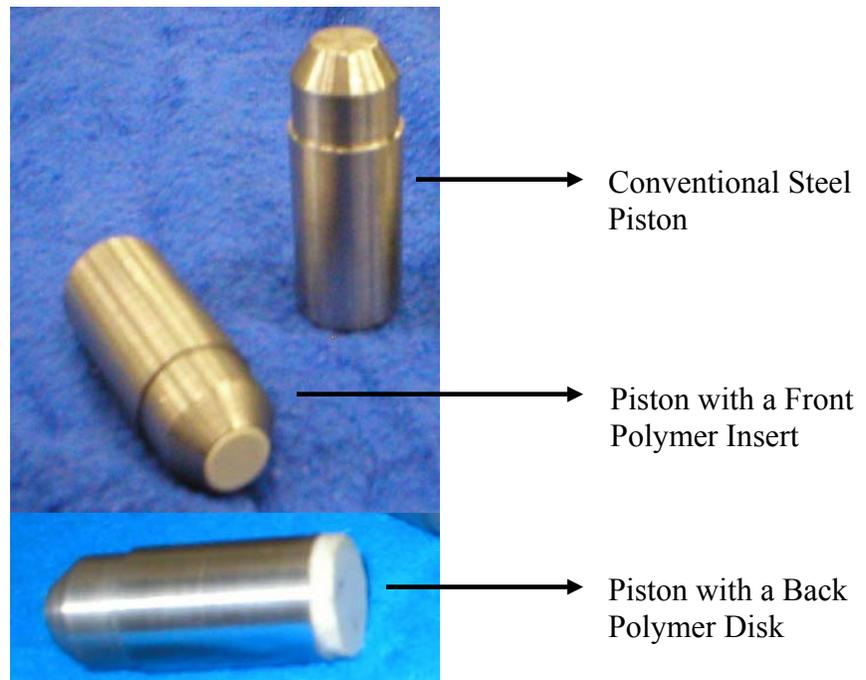
Figure 3.   Photographs of fabricated pistons for proof of concept testing.

Operator comparison tests of tool system vibration yielded a consensus that the perceived level of discomfort to the hand-arm system was reduced with the prototype piston when compared to the commercial tool running in air (no cutting). This design improvement was quantitatively demonstrated by power tool sound testing. Sound level measurements provided supporting data that substantiated the perceived vibration attenuation. Table 1 summarizes the results from the preliminary proof of concept power tool sound testing. The results show that there were statistically significant (at the 95% confidence interval) reductions in both peak sound pressure and sound level from polymer integration. The assessment of decreased operator discomfort and measured reduction in sound demonstrated a basis that the potential for vibration transmitted to the hands and arms had been reduced using polymer components in power tools.

Table 1.   Summary of preliminary power tool sound testing conducted with 2 trials for each piston treatment. The letter next to each numerical result signifies the statistical difference at the 95% confidence level for the different piston treatments. Averages of sound measurements are given for testing done with a faced off chisel for a tool running, no cutting. Distance from power tool to microphone is 3 feet and the data acquisition sampling frequency is 60kHz.

Piston Treatment	Sound Pressure (Pa)	Sound Level (dB)
Conventional Piston	41.7 a^{sp}	126.6 a^{sl}
Piston with Front Polymer Insert	23.8 b^{sp}	121.8 b^{sl}
Piston with Back Polymer Disk	33.0 c^{sp}	124.5 c^{sl}

Piston prototype work and observations made during testing provided key groundwork to effectively guide the larger polymer integration study. Visual analysis of the duplicate pistons after testing revealed that harsh impact occurs between the piston front and shaft of the cutting accessory. In contrast with design requirements for typical piston component life, a chisel has shorter functional requirements and is frequently replaced by tool users during normal industrial use. While piston prototyping and testing provided a strong foundation for the study, the investigation revealed important design considerations of component life and tool performance evident when replacing steel with a reinforced polymer material. In recognition of tool component life requirements coupled with the frequent replacement of most tools during normal use, a crucial transition in the project focus was made from piston modification with polymer material to the design of a chisel accessory to include a reinforced polymer insert.

Chapter 3

MODELING OF A CONSTRAINED REINFORCED POLYMER INSERT

3.1   Nomenclature

E   = elastic modulus
σx = stress on the chisel wall
σy = stress on the chisel wall, in the same plane but perpendicular to σx
σz = stress in the direction of the chisel shaft
εx = strain on the chisel wall
εy = strain on the chisel wall, in the same plane but perpendicular to εx
εz = strain in the direction of the chisel shaft
v = Poisson's ratio
E'   = constrained elastic modulus (effective modulus)

3.2   Methodology

Previous studies have reported several performance benefits from fitting a steel chisel with a polymer cap when compared to a conventional hand-struck bare chisel. Figure 4 illustrates a conceptual view of a power tool chisel with a polymer insert. The analysis and testing described herein investigates the feasibility and performance benefits of a modified accessory chisel including a polymer insert. First, a simple mass-spring analog is developed to obtain mathematical formulation of the governing equations of motion of the piston-chisel system. The model is used to design the polymer insert geometry and configuration based on stresses in the chisel tool end with a polymer. Furthermore, the model allows for the assessment of the force transmission characteristics of chisels for different insert materials in order to develop material property requirements to select a suitable high-performance reinforced polymer. Second, laboratory experiments are performed using a hydraulic Instron™ test machine to

measure force transmission and polymer integrity for prototype chisels as a function of the number of impacts (i.e. loading cycles). Third, field testing is conducted to measure vibration and noise from conventional and modified power tools to quantify potential biomechanical benefits of vibration and sound reduction to the tool user.
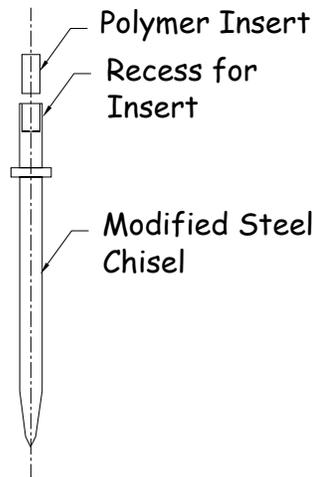
Figure 4. Exploded view of a steel chisel with a reinforced polymer insert.

3.3   Design of a Polymer Insert

From the previous discussion, the impact that occurs between the piston and the top of the chisel is the main source of high frequency vibration generation in the tool system. This zone of impact becomes the key area for design improvement within our study. To investigate the advantage of incorporating engineering polymers into power tool chisel accessory, a cylindrical insert was examined. The geometry lent itself for consideration in anticipation of simple integration with the existing shaft of the chisel. There were two proposed polymer insert configurations taken into account early in the project scope: 1) an unconstrained cylindrical insert to be sandwiched between the piston and chisel, and 2) an insert constrained within the end of the chisel housing. Modeling

was conducted to examine possible performance advantages of the unconstrained as well as the constrained insert designs.

Previous work with polymer capped, hand-struck chisels demonstrated that the stiffness of the polymer must be high in order to transmit and exert high forces onto the target thus preserving tool performance. Assuming the insert can be modeled as an axially loaded cylindrical plug, the stiffness can be computed as:

$$k = E\,A\,/\,t \qquad (1)$$

where,

E = polymer modulus
A = cross section area
t = polymer thickness in impact zone
k = cap stiffness

As expected, the polymer modulus must be high to insure high stiffness and peak impact force transmission. However, it is anticipated that the impact resistance must also be high to insure durability. The tradeoff between stiffness and durability will be discussed in more detail a later section.

Within the elastic limit of the material, there is a linear relationship between displacement and the force attempting to restore the material to equilibrium. Hooke's law defines the general relationship between stress and strain in the mechanics of materials,

$$\sigma_x\,/\,\varepsilon_x = E \qquad (2)$$

The constrained compression in one direction on the polymer insert, illustrated in Figure 3, can be characterized by 3-D Hooke's Law for isotropic materials,

$$\varepsilon_x = \frac{1}{E}\left[\sigma_x - v\left(\sigma_y + \sigma_z\right)\right] \quad\quad (3)$$

$$\varepsilon_y = \frac{1}{E}\left[\sigma_y - v\left(\sigma_x + \sigma_z\right)\right] \quad\quad (4)$$

$$\varepsilon_z = \frac{1}{E}\left[\sigma_z - v\left(\sigma_x + \sigma_y\right)\right] \quad\quad (5)$$
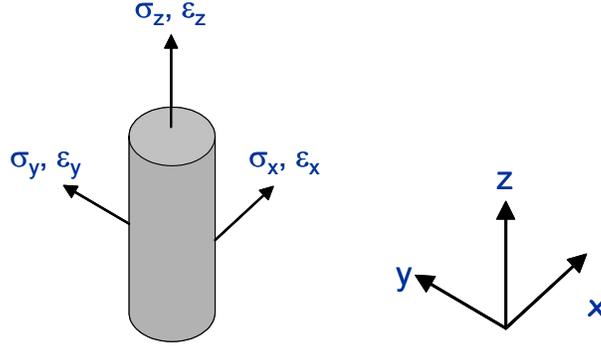
Figure 5.   3-D elemental loading of the constrained polymer insert.

If constrained in x and y,

$$\varepsilon_x = \varepsilon_y = 0 \quad\quad (6)$$

then,

$$\sigma_x = v\left(\sigma_y + \sigma_z\right) \quad\quad (7)$$
$$\sigma_y = v\left(\sigma_x + \sigma_z\right) \quad\quad (8)$$

and assuming uniform stress distributions on top of and around the cylinder, $\sigma_x = \sigma_y$ and for $v \neq 0$ then,

$$\sigma_z = \left(\frac{E}{1 - \dfrac{2v^2}{1-v}}\right) \quad\quad (9)$$

The relation between no radial strain and equal stresses in the planar directions parallel to the face surface of the insert yields an "effective" modulus for constrained polymer insert compression,

20

$$E' = \frac{E(v-1)}{2v^2 + v - 1} \qquad (10)$$

Note that the effective modulus is a function of the elastic modulus of the polymer

material (E) as well as the volume change needed for stress analysis which is indicated by

Poisson's ratio (*v*). Both material property values for polymers of interest were obtained

from Dupont Product Information Guides, available online [6].

The derivation for the imposed loading condition demonstrates that constrained

polymer insert performance is not only dependent on the material's stiffness; the effective

modulus is influenced by the directional deformation characteristics of the polymer.

Engineering materials have Poison's ratios between 0 and 0.5, with steels in the region of

0.3. Cork, a common bottle stopper, has a value near 0 while materials like rubber that

are almost incompressible approach the upper limit of 0.5. For simple compression,

viscoelastic materials like engineering polymers withstand pressure and expand when

compressed to preserve volume as a result of changing length. Figure 6 shows that

higher Poisson's ratios demonstrate greater increase in effective modulus as a result of

the constrained insert design. The side chisel walls of the constrained insert

configuration prevent this Poisson's effect from occurring. Therefore, this constrained

modulus is much larger than Young's modulus for the simple unconstrained insert

compression when the Poisson effect is free to occur, as illustrated in Table 2. It is

anticipated that the higher apparent modulus of the constrained polymer will provide

significant advantages in terms of force transmission in the tool.
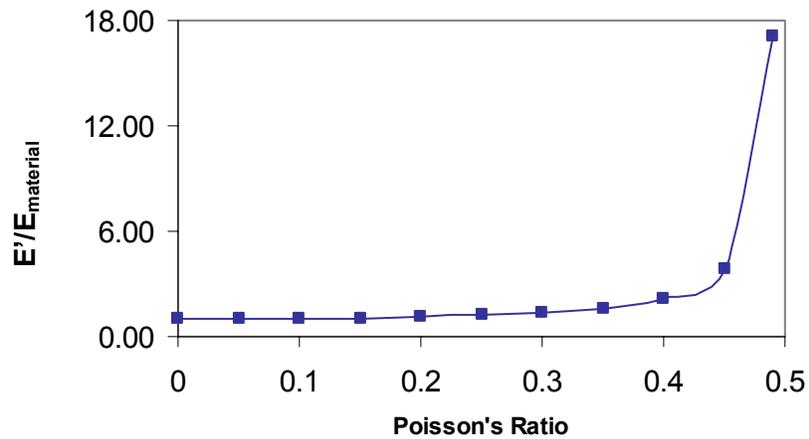
Figure 6. Predicted Effective Modulus curve for a commercially available polymer material vs. Poisson's ratio. As the Poisson's ratio for a polymer approaches that of an ideal incompressible material (volume does not change regardless of the applied stress), the effective elastic constant approaches infinity.

Table 2. Summary of calculations for effective polymer modulus resulting from the constrained insert configuration. The steel material of a conventional chisel has a Poisson's ratio, $v = 0.28$, and an Elastic Modulus, $E = 206.9$ GPa.

Polymer Insert Material	Poisson's Ratio, v	E (GPa)	E' (Gpa)	Increase in Modulus Value
Minlon™	0.40	5.2	11.2	114%
Hytrel™	0.45	0.6	2.2	279%

Chapter 4

MODELING OF THE FORCE TRANSMISSION CHARACTERISTICS WITH A POLYMER INSERT

4.1 Nomenclature

x1 = displacement of piston (from just touching back spring)
x2 = displacement of chisel (from just touching "stop")
x3 = velocity of piston
x4 = velocity of chisel
xa = piston reversal point
xi = sharpness parameter
tsec = time (sec)
m1 = piston mass
m2 = effective chisel mass
kb = back spring
kp = effective spring constant of piston and insert
kpa = spring constant of entire piston
kpb = spring constant of insert
kstop = max stiffness of retaining spring
F1 = reaction force on back of piston
F2 = compressive force on top of chisel
Fp = compressive air force on back of piston
Fs = retaining spring force on chisel
Fw = reaction force of "work" being cut
F_R = residual force used to normalize forces (N)
L = length used to normalize lengths (m)
T = time used to normalize time (sec)
y1 = dimensionless force on back of piston
y2 = dimensionless force on front of piston
yw = dimensionless force on work
yp = dimensionless net pressure force on back of piston
ys = dimensionless retainer spring force

4.2 Model Development

Figure 7 below illustrates the key elements used in the spring-mass model of a reciprocating piston impact tool system.
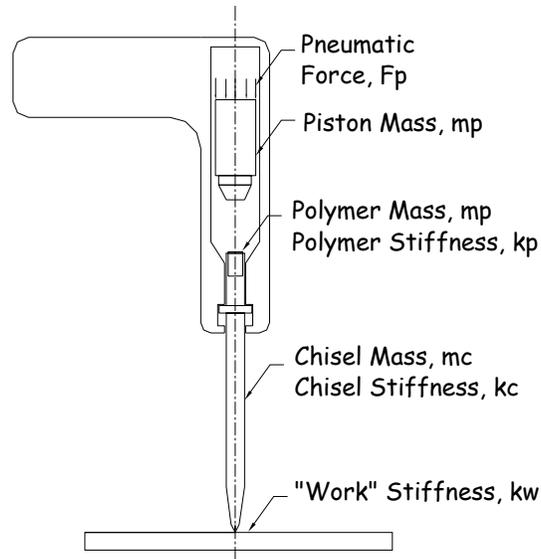
Figure 7. Mass and spring elements used to model the pneumatic tool impact system.

An analysis was made using the following assumptions:
- The force from the air pressure is modeled using the hyperbolic tangent function with the sharpness parameter, x_i.
- There is no negative chisel displacement.
- Poisson's ratio is not modeled as time dependent.
- Parameter k_p is the effective spring constant for the springs in series modeling the stiffness for the piston and polymer insert components.
- No coulomb friction or dampening contributed to energy lost during component motion and impact.
- The mass of the chisel and the spring constant of the work are key parameters in simulating the chisel force output.
- Deformations are linear elastic and kinetic energy is lost to the work, k_w, when the chisel is retracting (chisel velocity is negative).

The following were identified as inputs to the model:
- Chisel modulus, top shaft diameter, length, density (steel)
- Piston weight, modulus, front diameter, back diameter, length
- Insert modulus, Poisson's ratio, diameter, length, density
- Spring constant of work
- Compressed air pressure

The outputs of the model were then defined as:
- Effective chisel weight
  [calculated from chisel and insert density and volume]
- Displacement vs. time for the piston
- Velocity vs. time for the piston
- Output force vs. time for the top of the chisel

- Output force vs. time for the bottom of the chisel
- Effective polymer spring constant
- Effective modulus for the insert
- Max force on the top of the insert and the bottom of the chisel

4.3   Mathematical Formulation

Using the above definitions and summing the forces acting on each mass, the equations of motion for the piston and chisel are respectively,

$$F_1 = m_1 \ddot{x}_1 + F_2 - F_P \tag{11}$$
$$F_2 = m_2 \ddot{x}_2 + F_W + F_S \tag{12}$$

where the force due to the air pressure is,

$$F_P = \left(PA \tanh\left((a - x)\xi\right)\right) \tag{13}$$

and the contact forces, retaining spring force, and reaction force due to the "work" being cut, respectively, are,

$$F_1 = MAX(-k_B x_1, 0) \tag{14}$$
$$F_2 = MAX(k_P(x_1 - x_2 - L), 0) \tag{15}$$
$$F_S = MIN(k_{stop} x_2, F_R + k_R x_2) \tag{16}$$
$$F_W = k_W x_2 \tag{17}$$

and the effective spring constant for polymer insert and steel chisel stiffnesses (i.e. two springs in series) is,

$$k_P = \cfrac{1}{\cfrac{1}{k_{Pa}} + \cfrac{1}{k_{Pb}}} \tag{18}$$

Combining the above equations gives the ordinary differential equations for the tool system with the specified boundary conditions,

$$\ddot{x}_1 + \frac{k_P}{m_1}(x_1 - x_2 - L) - \frac{PA}{m_1} \tanh((a - x)\xi) + \frac{k_B}{m_1} x_1 = 0 \tag{19}$$

$$\ddot{x}_2 + \frac{k_w}{m_2} x_2 + \left(\frac{F_R + k_R x_2}{m_2}\right) - \frac{k_P}{m_2}(x_1 - x_2 - L) \tag{20}$$

$$x_1(0) = x_2(0) = \dot{x}_1(0) = \dot{x}_2(0) = 0 \tag{21}$$

These equations can be normalized for computational simplicity. Defining the following,

$$T = \sqrt{m_2 / k_R} \qquad\qquad (22)$$
$$F = L k_R \qquad\qquad (23)$$
$$a = F_R / F \qquad\qquad (24)$$
$$b = PA / F \qquad\qquad (25)$$
$$c = m_1 / m_2 \qquad\qquad (26)$$
$$d = x_a / L \qquad\qquad (27)$$

gives the final dimensionless equations that describe the equations of motion of the piston and chisel illustrated in Figure 6,

$$\ddot{x}_1 + y_2 - y_P - y_1 = 0 \qquad\qquad (28)$$
$$\ddot{x}_2 + y_W + y_S - y_2 = 0 \qquad\qquad (29)$$
$$y_1(0) = y_2(0) = \dot{y}_1(0) = \dot{y}_2(0) = 0 \qquad\qquad (30)$$

4.4   Simulation of the Piston and Chisel Motion and Forces

The differential equations were solved in vector matrix form using *Matlab*™

software. See Appendix A for the complete *Matlab*™ simulation code. The nonstiff

function ODE45 was used to integrate the system of differential equations y' = f(t,y)

from time T0 to TFINAL with initial conditions Y0. Each row in the numerical solution

array corresponds to a variable time returned in the column vector T. Most input

parameters were determined by physical measurement. Only two parameters – the

sharpness factor of the hyperbolic function and the ratio of air flow reversal point to total

piston stroke length – were adjusted to ensure complete reciprocating motion of the

piston. The complete set of base case parameters are documented in Table 3.

Table 3.   Parameter values used in simulations.

Parameter	Value used in Simulations
Piston Weight	93.0 g
Piston Diameter	1.89 cm
Piston Length	4.60 cm
Piston Stroke Length	5.96 cm
Chisel Top Shaft Diameter	1.01 cm
Effective Chisel Length	24.8 cm
Insert Diameter	Design Variable
Insert Length	Design Variable
Steel Density	$1.0E\text{-}06$ N/m^3
Steel Modulus	206.9 GPa
Minlon™ 11C40 Density	$2.0E\text{-}07$ N/m^3
Minlon™ 11C40 Modulus	5.2 GPa
Minlon™ 11C40 Poisson's Ratio	0.40
Hytrel™ 7246 Density	$1.7E\text{-}07$ N/m^3
Hytrel™ 7246 Modulus	0.57 GPa
Hytrel™ 7246 Poisson's Ratio	0.45
K_r, Retaining Spring Constant	25 kN/m
K_w, "Work" Spring Constant	87563 kN/m
F_r, residual spring force	30.6 N
Compressed air pressure	621 kPa

By developing and solving the governing equations of motion for the piston-chisel system, a mathematical simulation has been achieved for use as a design tool. A number of outputs as a function of time have been computed to characterize the cyclical nature in terms of position and force output of the tool system. The simplest degree of validation for the model can be demonstrated without any physical testing of tool performance. The 56 Hz simulated frequency for the piston in the conventional tool system closely matches the 58 Hz frequency rating provided in the tool manufacturer's product specification literature. Figures 8a through 8c are typical time graphs of simulation outputs for one impact cycle with the prototype chisel.

Piston Displacement vs. Time (a)

Piston Velocity vs. Time (b)
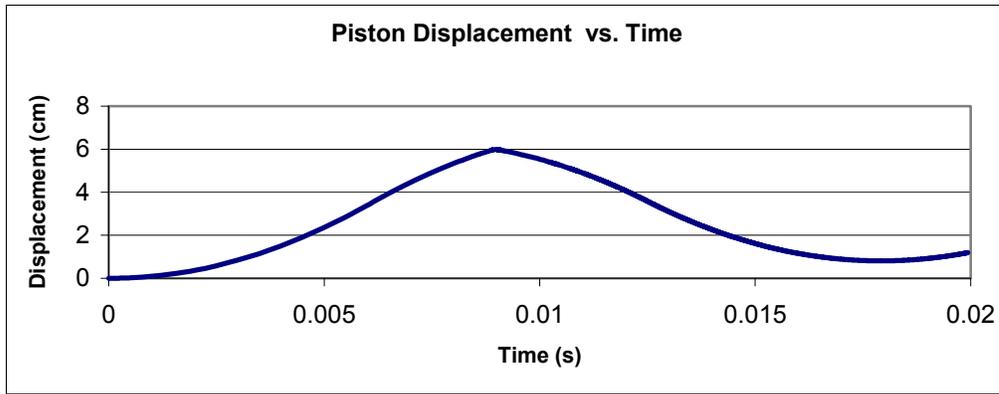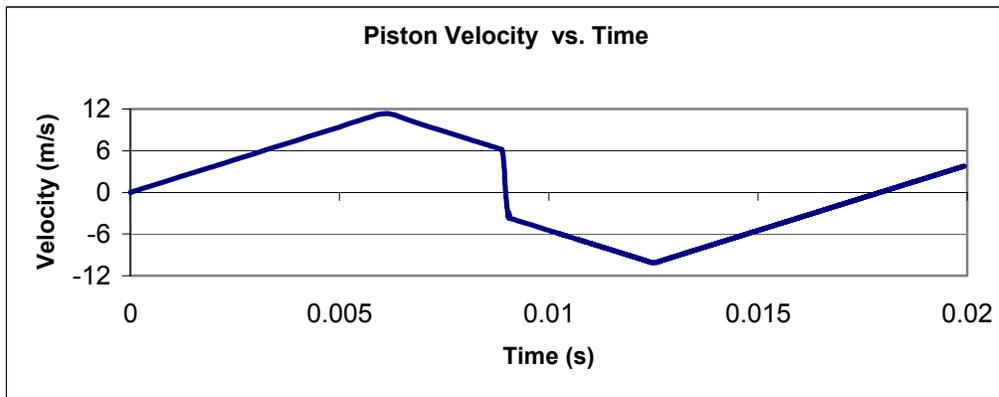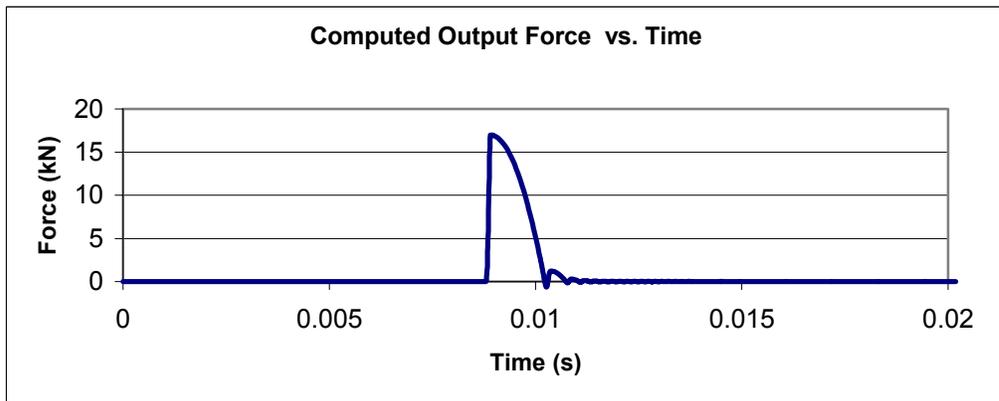
Computed Output Force vs. Time (c)

Figure 8. Simulation outputs of (a) piston displacement, (b) piston velocity, and (c) chisel output force characterizing the behavior of a conventional pneumatic tool for one impact cycle. Actual tool response is cyclical.

As the piston makes its forward stroke down the tool chamber, the chisel remains in a fixed position. At maximum piston displacement, there is a spike in the chisel output displacement and force due to the impact between the piston and chisel. Following this collision, the piston reverses direction and the chisel moves back as the retaining spring retrieves the chisel to its original position. The plot of piston velocity also demonstrates the sudden directional change of the piston (positive to negative velocity) upon impact with the chisel. See Appendix B for complete simulation outputs as a function of time for a prototype chisel with a polymer insert.

In addition to *Matlab™* simulations, calculations based upon the conservation of energy and impulse momentum theorems provided further supporting evidence to make a strong order of magnitude prediction for the tool output force. See Appendix C and Appendix D for complete documentation of each computation, respectively. The results of this analysis support the simulation results by estimating the chisel output force on the order of 10 kN.

4.5   Prediction of Chisel Cutting Force During an Impact

Table 4 summarizes the results of simulated force for the top and the bottom of the chisel. In each case, the forces shown are for both a conventional chisel and a chisel with a polymer insert. The force on the bottom is most relevant since it is the force actually cutting into the work. The slight difference seen in the simulated force values between the top and bottom of the chisel demonstrates the effect of the chisel inertia. While chisel inertia slightly reduces predicted values of force transmission between the top and bottom of the chisel in both scenarios, the maximum chisel forces for the

29

conventional chisel are only slightly higher than the forces predicted for the chisel with a

constrained Minlon™ polymer insert. Force vs. time is plotted on Figure 9 for the force

at the bottom of the chisel.

Table 4. Summary of maximum predicted forces for various chisel configurations.
For the chisels with a polymer insert, the insert has been modeled with a
geometry of L = 1.5 centimeters and d = 0.72 centimeters.

Chisel Treatment	Force at Top of Chisel (kN)	Force at Bottom of Chisel (kN)
Conventional Steel Chisel	17.00	16.99
Chisel with Minlon™ Insert	14.11	13.92
Chisel with Hytrel™ Insert	6.18	6.08
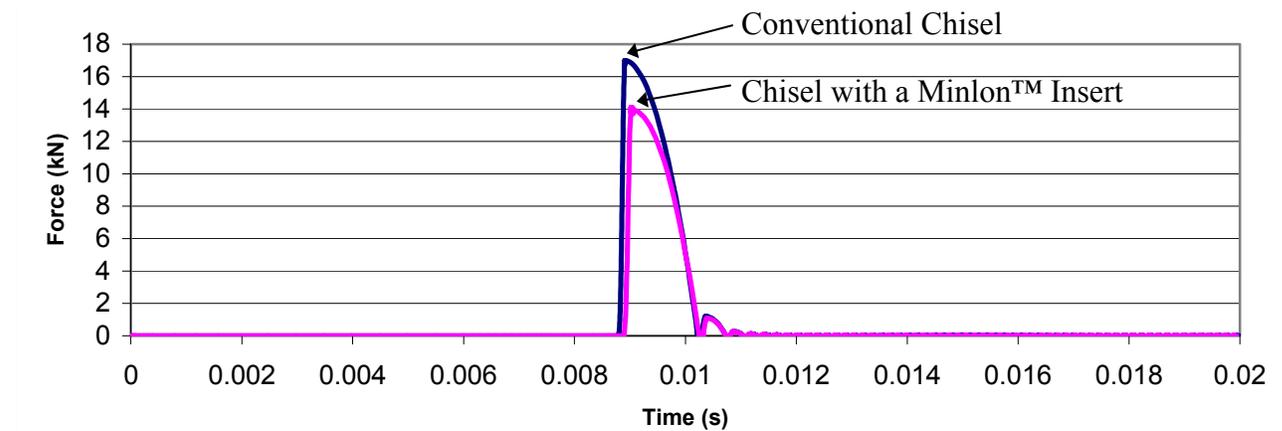
Figure 9. Predicted force vs. time graphs for the force at the bottom of a
conventional chisel and a chisel with a polymer insert.

4.6   **Effect of Polymer Material Properties on Maximum Output Force**

Maximum chisel force is the key parameter for tool performance, therefore, the

polymer modulus-force relation has been examined. Higher modulus polymers yield

higher effective modulus values (see Table 2). It is expected that increasing the effective

polymer modulus will increase the maximum chisel force achieved. Maximum force is

plotted against the polymer modulus normalized by the modulus of steel in Figure 10. A

log scale has been used to demonstrate a range of polymer materials. Constrained

compression increases the effective stiffness of a polymer which leads to a beneficial

gain in output force.
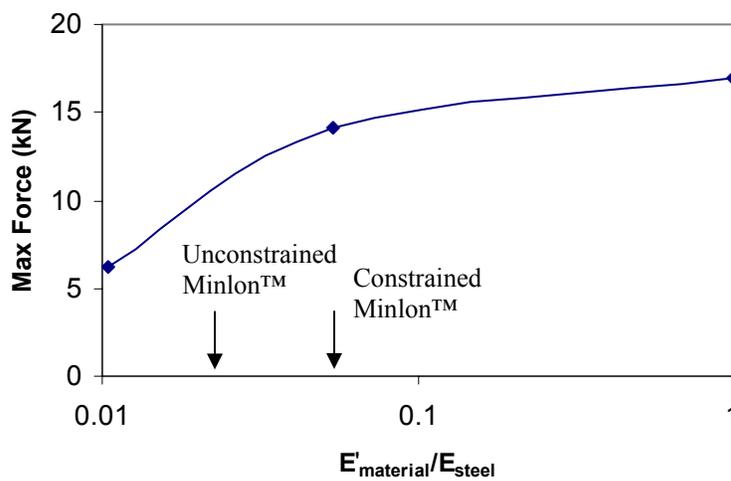
Figure 10.   Effect of insert modulus on the maximum predicted chisel force.

Two key learning points result from this evaluation. First, the modulus of high

impact polymer materials can be increased by constraining inserts within the chisel

housing. Second, polymer inserts with a high effective modulus produce a maximum

output force that is close to that of a conventional chisel accessory. The more stiff and

incompressible (less elastic) a polymer material, the greater the maximum chisel force.

4.7   Model Validation

Laboratory testing was used to validate the accuracy of the force predictions. A

load cell was used to quantify the peak force exerted on a 6.35 mm drill rod on a hard

surface by the cutting tool. Table 5 compares the predicted maximum output force

exerted by the chisel to the measured value of force. The measured values of force for

both a conventional chisel and a chisel with a polymer insert are similar to the simulation

results. As expected, the mean value results show that a polymer insert reduces chisel

force, however, this reduction was found to be statistically insignificant (at the 95%

confidence level).

Table 5. Summary of predicted and measured force exerted on the test specimen by the chisel. There was a small but statistically insignificant decrease in measured force output for a prototype chisel when compared to the output force value for a conventional chisel.

Treatment	Predicted Force (kN)	Measured Force (kN)		
	from *Matlab* ™	Lower 95% Bound	Mean	Upper 95% Bound
Conventional Steel Chisel	16.99	14.94	16.1	17.28
Chisel with a Minlon™ Insert	13.92	10.68	14.3	17.83

4.8   Effect of Insert Diameter and Insert Length

Increasing polymer stiffness certainly increases chisel force. For the conventional

chisel system, the model predicted a maximum output force of 17 kN. The model can

also be used to optimize the chisel and a polymer insert geometries, particularly with

respect to the choice parameters of insert length and insert diameter to achieve desirable

chisel forces. From Equation 1, it is expected that polymer stiffness can be improved by

increasing insert diameter (which increases cross sectional area). It is also anticipated

from the stiffness equation that increasing insert length reduces insert stiffness.

The effect of polymer insert length was computed and plotted on Figure 12. The zero insert length level corresponds to a conventional chisel. As expected, increasing polymer length decreases maximum force. Longer polymer inserts are not as stiff as shorter inserts of the same diameter.

The effect of insert diameter on various insert lengths (Figure 12) results in a relation similar to the modulus effect predicted on Figure 10. Maximum chisel cutting force increases as insert diameter increases and insert length is reduced. In other words, as the geometry of the insert increases polymer stiffness, the exerted output force from the chisel is higher. The zero insert diameter level corresponds to the maximum force output of a conventional chisel.
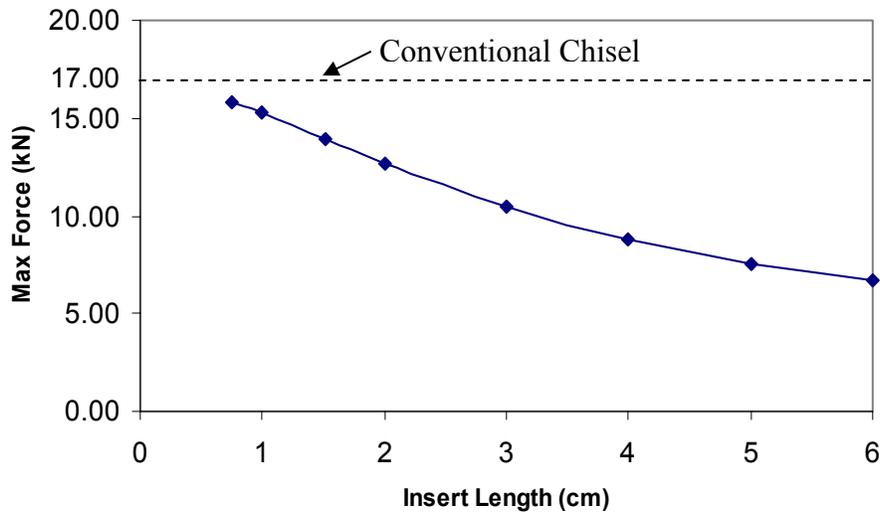
Figure 11. Predicted maximum force for a chisel with a polymer insert vs. insert length. The plot shown is for an insert with a constant diameter of 0.72 centimeters. The dashed line specifies the predicted peak force for a conventional chisel.
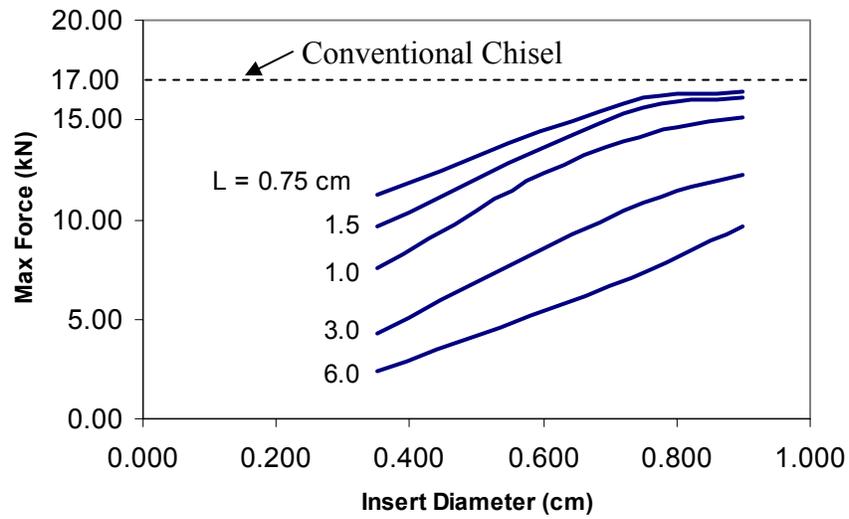
Figure 12. Predicted effect of insert diameter and length on maximum chisel force of a chisel with a polymer insert. The predicted maximum output force for a conventional chisel is indicated by the dashed line.

Chapter 5

DURABILITY AND PERFORMANCE TESTING

In this chapter, two methods of testing are described. Laboratory testing using an Instron™ test machine is performed to artificially aged the polymer insert with repeated loading cycles. Test results are used to confirm the effective modulus of the insert and understand the life-load behavior (i.e. the durability) of the polymer insert. In addition, field (human) trials in which a pneumatic chisel equipped with a chisel and polymer insert are conducted to measure the vibration and sound emission characteristics of the prototype tool.

5.1   Methodology for Insert Material Integrity Testing

High frequency Instron™ testing was used to reproduce controlled impact cycles for laboratory testing and observation of chisel prototype behavior. The specific objectives of the testing were to determine force transmission and polymer degradation as a function of the number of impact cycles at comparable loads applied to the chisel accessory in the running tool. Characterizing the fatigue life of materials is dependent upon the damage of cumulative cycles, not the frequency of the loading. Therefore, the frequency of impact is a secondary test parameter to the desired load and number of cycles to be applied during testing.

Prototype chisels were mounted in an Instron™ hydraulic test machine shown in Figure 13 for artificial aging due to cyclical loading. The top portion of the prototype chisel is exposed when mounted for testing. The testing machine applied a regular

sinusoidal load cycling between 0.89 kN and 12.5 kN at 15 Hz for up to a million cycles.

Modulus values were estimated from load-deformation data.

(a)

(b)
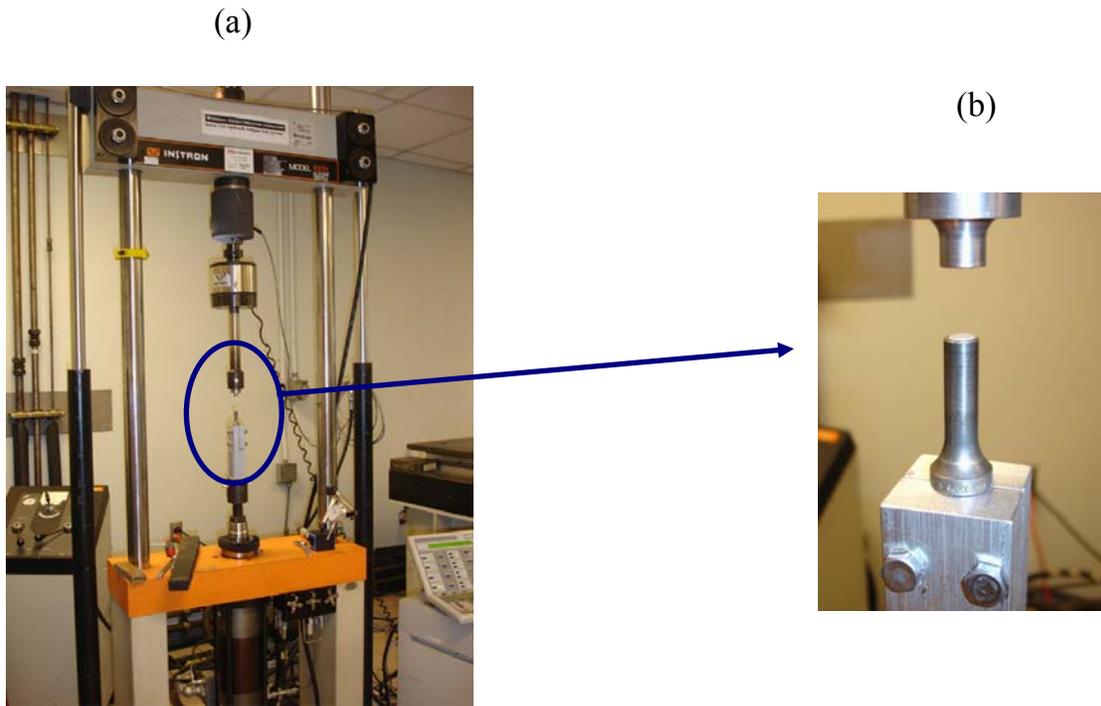
Figure 13.   The prototype chisel is held in a fixture during Instron™ machine laboratory
testing (a). The top of the chisel remains exposed (b) for all tests.

5.2   Measured Insert Stiffness (Modulus)

The measurement of stiffness for a material can be approximately calculated

relative to the measurement of directional deformation. This rate of change of stress with

strain can be determined experimentally from the slope of a stress-strain curve. Tests

were conducted for a chisel with a new Minlon™ insert and a chisel with a Minlon™

insert aged by Instron™ loading. Figure 14 shows a stress-strain plot for a chisel with a

new Minlon™ insert. The average computed modulus for each insert test condition is

summarized in Table 6. The results show that there was a small but significantly

insignificant increase (at the 95% confidence interval) in the insert stiffness for the

artificially aged insert. Photographs of the top of the chisel with a polymer insert prior to

Instron preloading and after Instron preloading are shown in Figure 15.
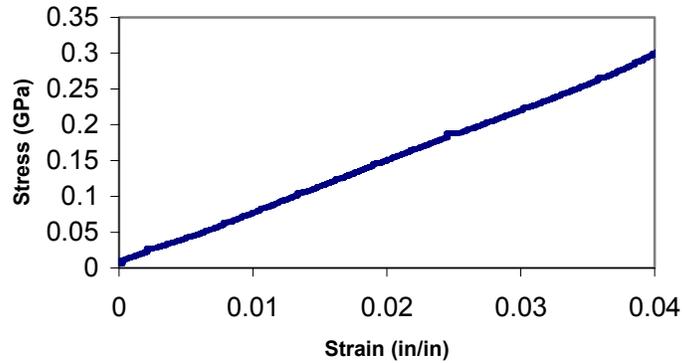
Figure 14. Typical stress-strain graph of new Minlon™ insert. Processing for an
average modulus (stiffness) value was achieved by computing the slope of a
trendline for the middle two-thirds of collected data.

Table 6. Summary of measured polymer insert modulus values for 10 trials.
Averages and the range of responses are given.

	New Insert	Preloaded Insert
Modulus Value (GPa)	6.94 a (6.27 to 7.24)	6.86 a (5.83 to 7.52)

(a)   (b)
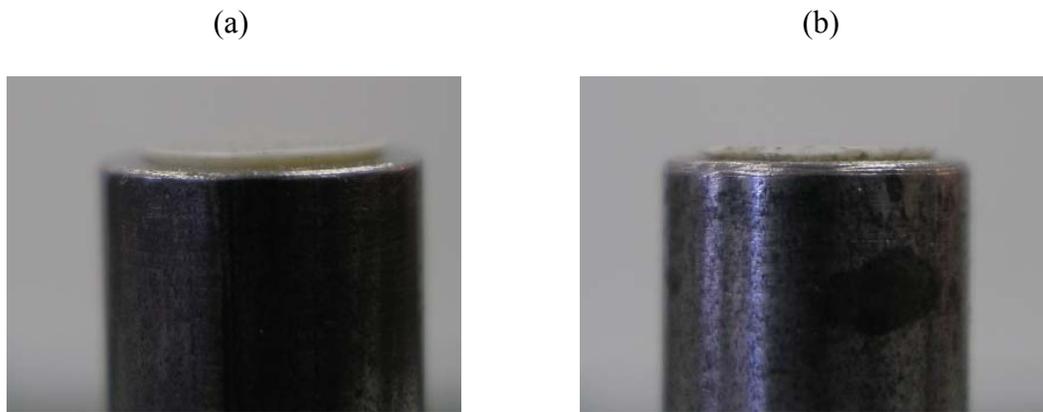
Figure 15. Photographs for the top portion of a prototype chisel with a Minlon™ insert (a) prior to Instron™ testing and (b) after preloading in the Instron machine.

The experimental technique and methodology used to preload an insert with the Instron machine is accurately controlled and yields repeatable results. While a preload did not significantly increase the stiffness of the polymer insert, the cyclical loading did contribute to the survivability of the insert during later tool use. A "geometric effect" imposed during cumulative Instron preloading improves insert life of the exposed polymer material. Experimental testing of prototype chisels run in a tool without preloading resulted in the quick disintegration of unconstrained polymer material. Preloading a polymer insert elongates the effectiveness of the prototype configuration by postponing material dissipation during tool operation. As a result of preloading a chisel with a polymer insert, the prototype chisel survived running in the tool (no cutting) for 1 hour of time. While the exposed polymer is slightly compressed as a result of the combination of preloading and 1 hour of tool use, the inverted conical frustum shape of the exposed insert remains preserved as seen in Figure 16.
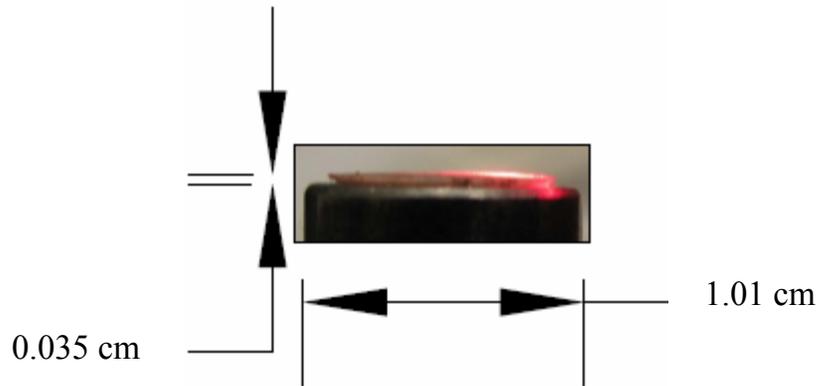
Figure 16. Top portion of a prototype chisel with a Minlon™ insert after Instron™
preloading and 1 hour of tool use. The length of exposed polymer prior to
preloading was 0.10 cm.

**5.3   Instrumentation and Data Acquisition & Analysis for Vibration and
Sound Emission Measurements**

Vibration measurements were made at the pneumatic chisel handle-hand interface

using a PCB Piezotronics Tri-Axial Accelerometer (Model SEN021F) with a nominal

sensitivity of 10 mV/g and a frequency response range of 1-10,000 Hz. A small

mounting fixture was used to position the accelerometer along the hand. Signal

conditioning for the accelerometers was accomplished with a PCB Piezotronitcs Model

480B21 Three-Channel Conditioner.

A LinearX 150 mm diameter precision acoustic measurement microphone (Model

M51A) with an acoustic sensitivity of 11.086 mV/94.00 dBspl was used for all tests. A

DC supply of 9 volts powered the calibrated microphone and a National Instruments Data

Acquisition Card (E-Series, PCMCIA 16-bit) and laptop computer were used to record

the sound signal along with the vibration signals.

A *LabVIEW* program was written to gather the data as well as process and analyze

the acquired signals for meaningful information (Figure 17). Periodic checks of the data

acquisition and signal processing system were accomplished with several different tone sources: a perfect "E" note tuning fork (329 Hz), and two *Projects Unlimited* continuous tone piezoelectric audio indicators (2800 and 4500 Hz).

Data was manipulated and analyzed in order to extract desired information and obtain results from the time domain signal acquired using the hardware and *LabVIEW* program. Fast Fourier Transforms were preformed on sound vs. time and acceleration vs. time data sets to determine and identify dominant components in the frequency domain.
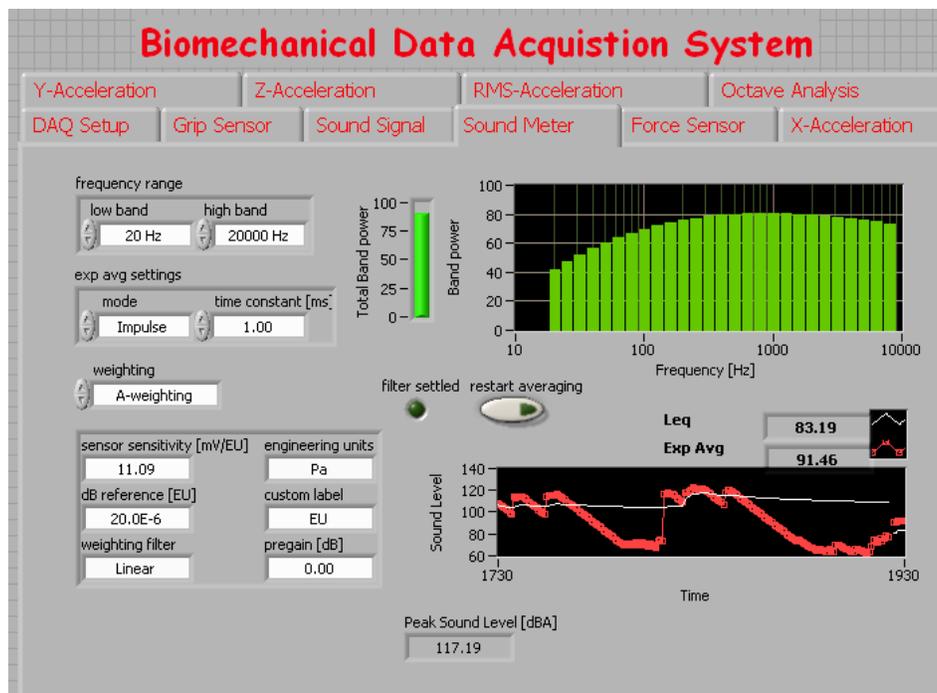
Figure 17. *LabVIEW* interface for the data acquisition and processing program used to collect and analyze the sound and vibration data.

In order to obtain peak decibel output readings, an exponential averaging technique was utilized. The averaged level of the sound pressure signal (measured in units of Pascal) was computed based on an exponential mode after each sample of time and returned as an exponential averaged sound level in decibels. Selecting a custom exponential time constant of 125 milliseconds allowed for the continuous running

average to accurately capture a short duration impulsive signal. Discrete Fourier

transforms of the sound pressure and acceleration were performed using the following

form:

$$F_n = \sum_{k=0}^{N-1} f(n)e^{i2\pi nk/N} \tag{4}$$

where,

F_n = Fourier transform
f(n) = n^{th} measured time domain data
N = Number of data

5.4   Analysis of Tool Sound Emission

The results of quantitative sound measurement recorded in decibel readings are

summarized in Table 7. The microphone was placed 1 m from the tool. A chisel with a

polymer insert was found to significantly reduce the continuous running average (Leq)

and exponential running average (Exp) of sound emission by the tool system. However,

a statistically insignificant reduction in peak sound pressure (dBA) was recorded for the

chisel with a polymer insert when compared to the conventional steel chisel.

Table 7.   Summary of sound testing for a chisel with a new Minlon™ preloaded insert
and a conventional chisel accessory. A total of 6 trials were conducted for
each treatment the high and low readings discarded prior to statistical
analysis. Averages responses are given for sound at a 1 meter distance.

Chisel Treatment	Leq (dBA)	Exp (dBA)	Peak Pressure (dBA)
Conventional Steel Chisel	108.8 a^L	106.6 a^E	126.9 a^P
Chisel with a Minlon™ Insert	106.6 b^L	104.4 b^E	125.3 a^P

Figures 18 and 19 contain typical sound pressure vs. time plots for a pneumatic

tool with a conventional chisel and chisel with a polymer insert, respectively. Analysis of

41

the frequency content of these signals as illustrated in Figures 20 and 21 suggests that a
chisel with a polymer insert reduces the sound emitted by a pneumatic chisel across the
frequency spectra, including harmful high-frequency noise.
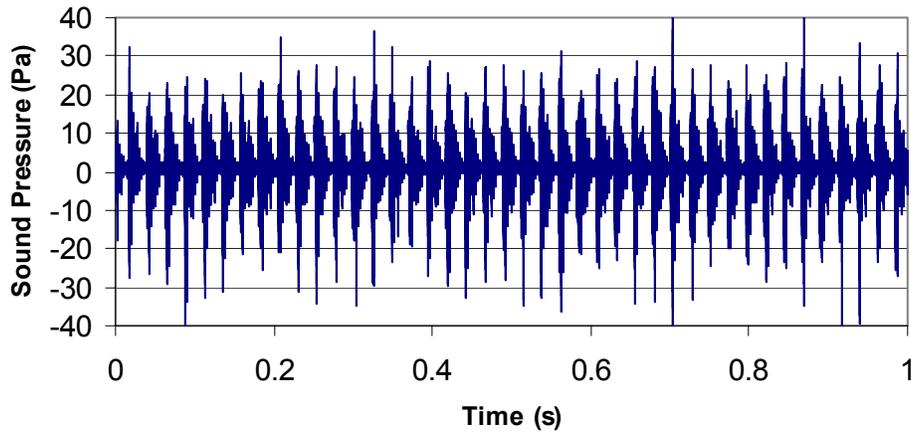
Figure 18. Typical time domain response of sound for a conventional chisel.
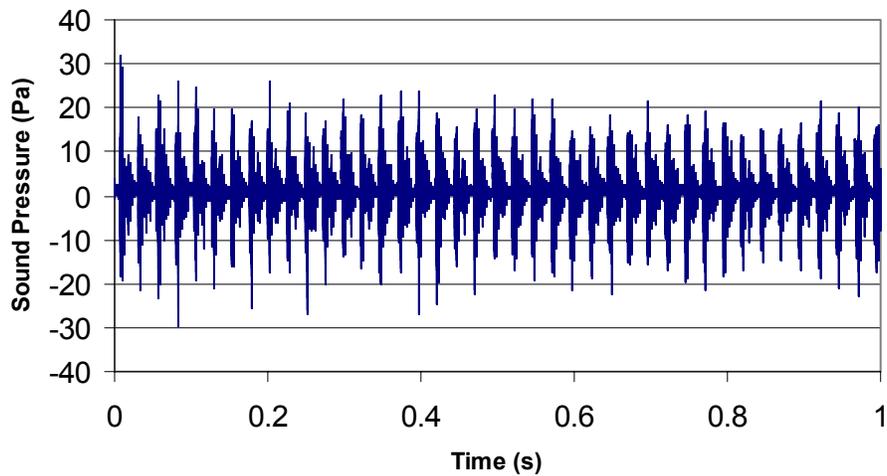
Figure 19. Typical time domain response of sound for a prototype chisel with a
Minlon™ insert.
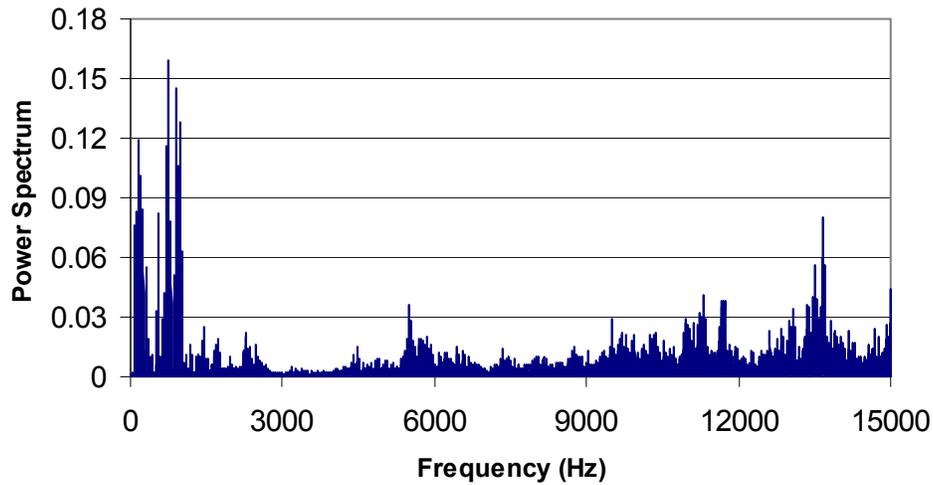
Figure 20. Frequency spectra of the sound pressure data in Figure 18 for the conventional chisel.
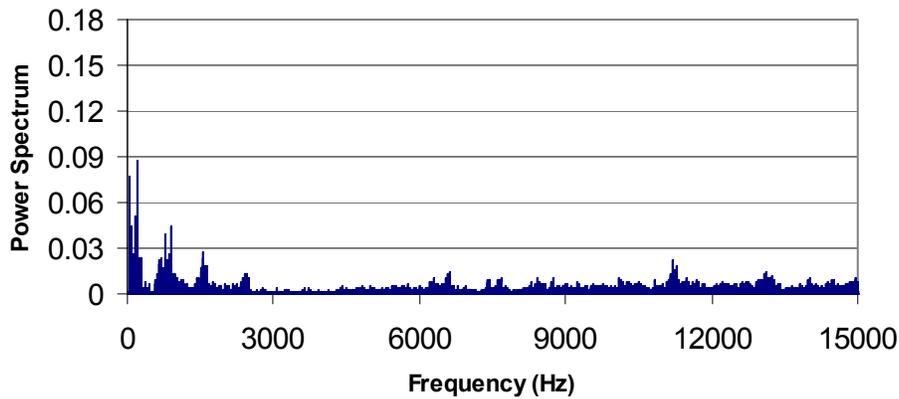
Figure 21. Frequency spectra of the sound pressure data in Figure 19 for a Prototype Chisel with a Minlon™ insert.

5.5   Analysis of Tool Vibration

To measure the vibration transmitted to the hand that was holding the pneumatic

tool, the triaxial accelerometer was mounted on the tool at the hand-handle interface.

Tests were conducted with a prototype chisel with a polymer insert in a pneumatic tool;

measurements were made with the tool cutting a 6.25 mm steel rod. A conventional

chisel without an insert was also tested as an experimental control.   In general, vibration

magnitudes were greatest in the axial direction (i.e. the direction of cutting) for all tests.

Figures 22 and 23 contain typical axial acceleration vs. time plots at the tool-hand

interface for a conventional chisel and a chisel with a polymer insert, respectively.

Examination of these graphs revealed that vibration in the axial direction was reduced by

a factor of 2. The axial direction is the direction in which the tool and piston travel, and

was the predominate direction of vibration in all tests.

For both the conventional and prototype chisel, there was significant high

frequency content associated with the tool between 4,000 and 6,000 Hz as illustrated in

Figures 23 and 24. Although the chisel with a polymer insert did not seem to shift this

regime of vibration to a lower frequency, the prototype chisel did reduce the magnitude

of the power spectrum. The low frequency vibration in Figures 24 and 25 corresponds to

the impact frequency of the internal piston component (rated at 58 Hz). The chisel with a

polymer insert did reduce the magnitude of accelerations at this low frequency as well.
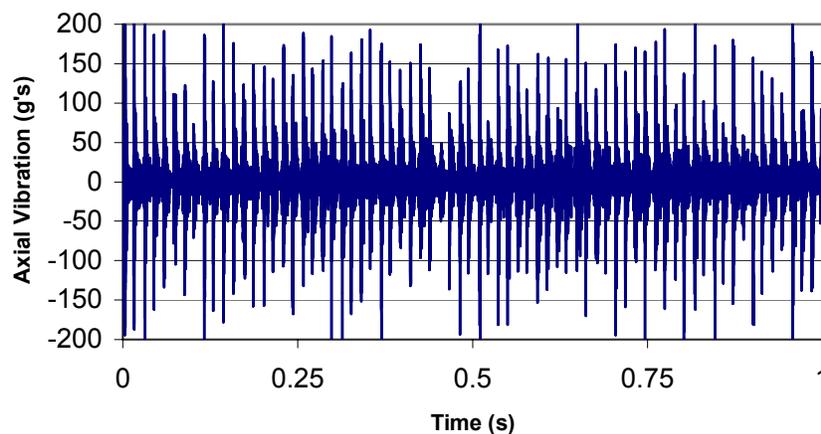
Figure 22.   Typical time domain vibration response in the axial direction at the *hand* for
a conventional chisel.

Figure 23. Typical time domain vibration response in the axial direction at the *hand* for a prototype chisel with a Minlon™ insert.

Figure 24. Overall frequency content of the data in Figure 22 for a conventional chisel.

Figure 25. Overall frequency content of the data in Figure 23 for a prototype chisel with a Minlon™ insert.

To determine the effects of the insert on vibration transmitted in the arm, tests were conducted in which measurements were made at the elbow. The triaxial accelerometer was mounted on the user's elbow using a small mounting fixture and zip ties. In all tests, the predominant magnitude of vibration was in the lateral direction; lateral is defined as the direction normal to the plane formed by the forearm and upper arm when bent at a right angle. Figures 26 and 27 contain typical lateral acceleration vs. time at the elbow while using the conventional and polymer insert chisels, respectively. The corresponding frequency spectrums for each tool configuration are provided in Figures 28 and 29. Like the measurements taken at the hand, vibration levels at the elbow were reduced with the polymer. However, power spectrums for both the conventional and polymer chisels reveal that only a single dominant frequency is present corresponding to the cycle frequency of the piston. Surprisingly, it appears that no high frequency components of vibration present at the hand (evident in Figures 23 or 24) are transmitted to elbow for either tool suggesting that most of vibration energy is absorbed in the hand and wrist.

Together, these results are encouraging since both low and high frequency components of vibration are being reduced by the polymer insert. This is especially important at the lower frequencies where the most blood vessel and nerve damage is believed to occur from long term exposure to continuous vibration.
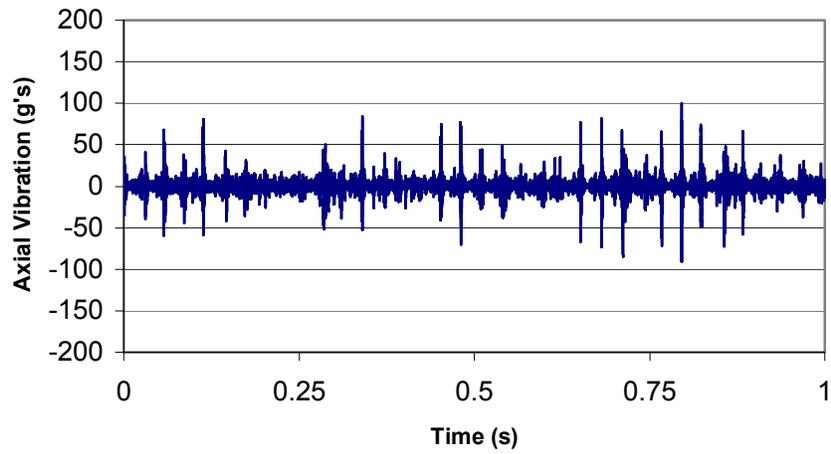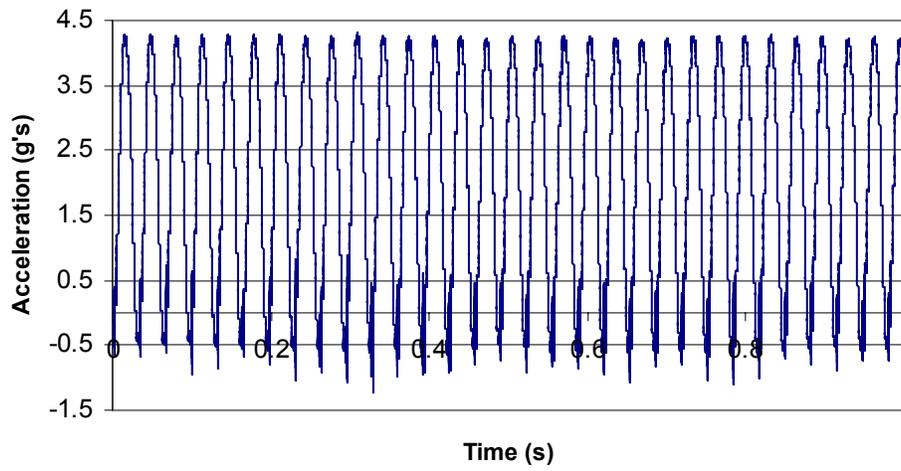
Figure 26. Typical time domain lateral vibration response at the *elbow* for a conventional chisel.
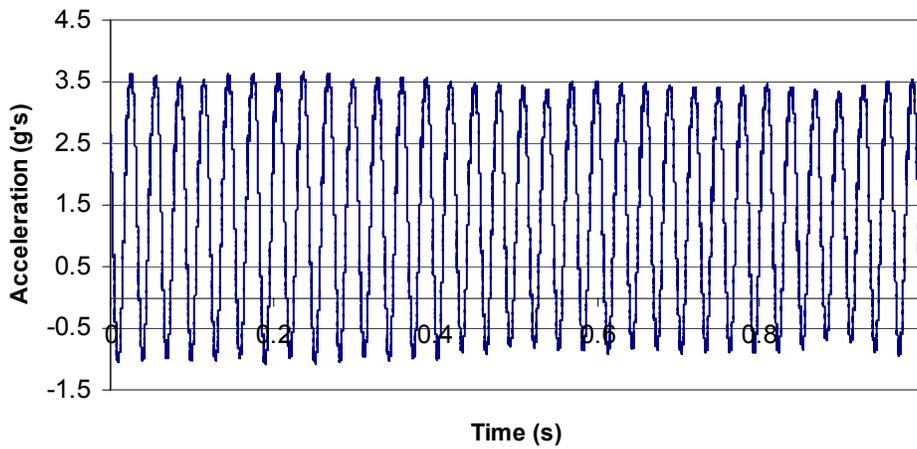
Figure 27. Typical time domain lateral vibration response at the *elbow* for a prototype chisel with a Minlon™ insert.
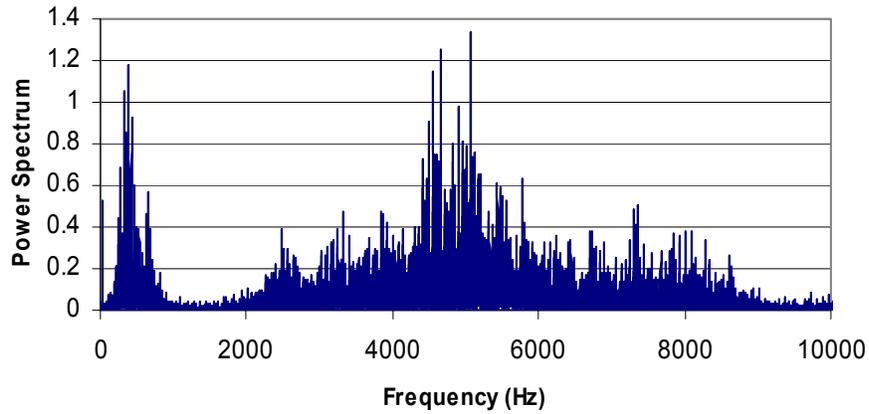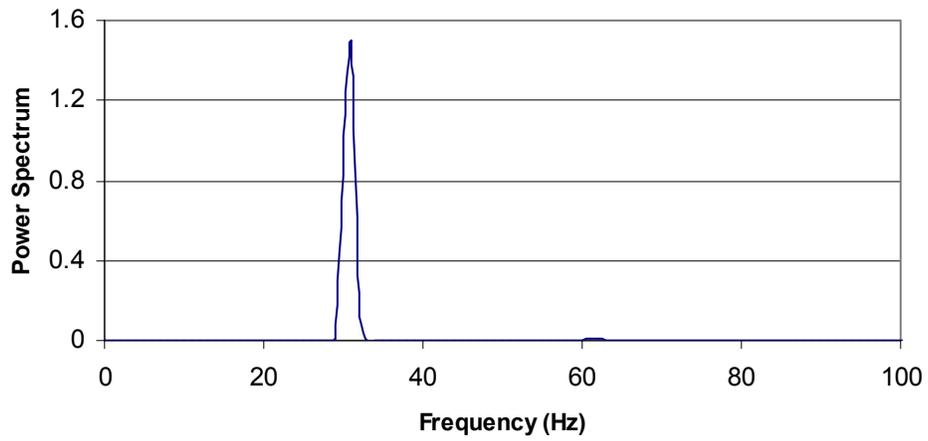
Figure 28. Overall frequency content of the data in Figure 26 for a conventional chisel.
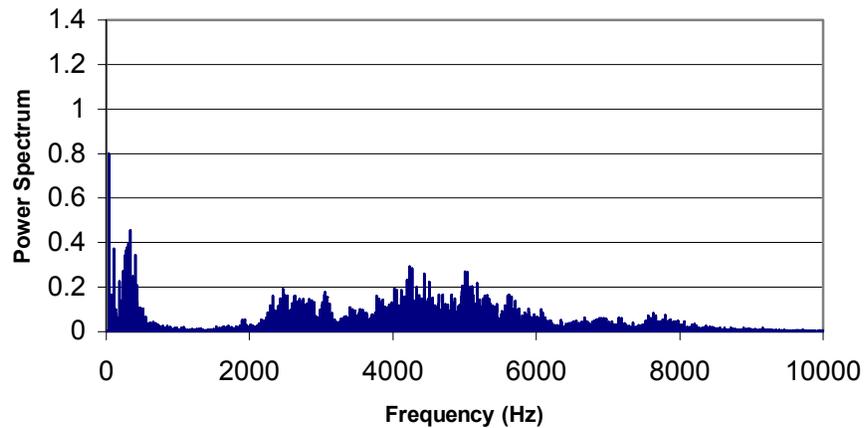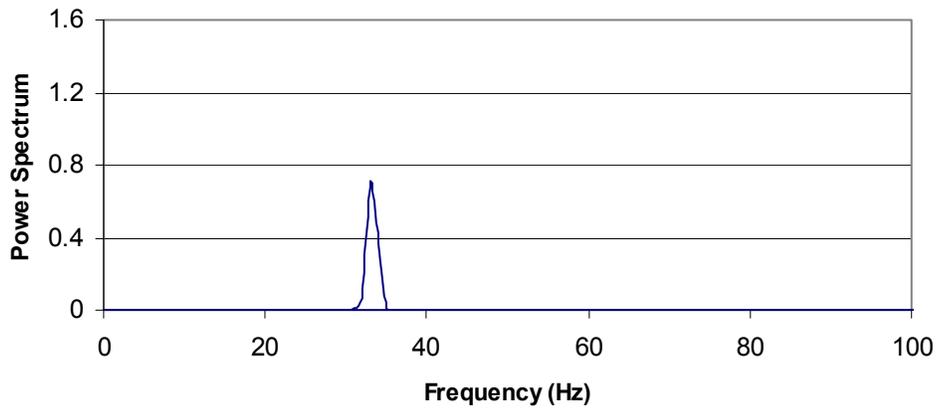

Figure 29. Overall frequency content of the data in Figure 27 for a prototype chisel with a Minlon™ insert.

Chapter 6

CONCLUSIONS & RECOMMENDED PATH FORWARD

6.1   General Discussion

Hand-arm vibration is a complex hazard resulting from a combination of environmental, individual, and ergonomic factors. Powered hand tools create an occupational risk for biomechanical injuries to many workers throughout the world whose jobs require frequent and continuous use of these devices. While administrative regulations, work practices, and personal protective equipment have been use to reduce the potential for some of the detrimental effects resulting from tool use, engineering controls and improved tool designs should be examined.

In light of the problems associated with the use of powered hand tools, a new chisel accessory design incorporating a reinforced polymer insert was investigated. A lumped-parameter model was used to simulate tool system behavior and compute force transmission characteristics of the new chisel design. Laboratory testing was also conducted to validate the model and quantify potential performance benefits in sound and vibration reduction resulting from a prototype chisel with a polymer insert.

6.2   Conclusions

Based on the results presented and analyzed in the study, the following conclusions have been made:

1. A mathematical simulation of the piston-chisel system has been developed and validated using first order differential equations.

2. Constraining and aging an insert as a function of the number of loading cycles increases the effective polymer modulus, E'.

3. Preloading a chisel with a polymer insert did not significantly increase insert stiffness, however, an increase in stiffness can be achieved through optimization of insert geometry (length, diameter).

4. Flexural modulus and Poisson's ratio of a polymer significantly effect force transmission characteristics of a chisel insert.

5. Predicted forces at the bottom of a chisel are similar to the experimentally measured chisel output forces. A polymer insert slightly reduces chisel force, however this reduction was found to be statistically insignificant at the 95% confidence level.

6. Prototype chisels with a Minlon™ insert significantly reduced the continuous running average of tool sound emission and decreased the magnitude of vibration transmitted to the hand by a factor of 2.

7. The use of polymers in power tool designs has the potential to reduce biomechanical injury and Hand-Arm Vibration related ailments to tool users. Specifically, the significant reductions in vibration, especially at lower frequencies where blood vessel and nerve damage is believed to occur, indicate the long term use of these new tools will likely prevent or delay the onset of vascular and nerve damage in the hand and arm if used properly.

8. Prototype chisels with a polymer insert have survived over 1 hour of field testing.

6.3   **Suggestions for Future Work**

The parameters of flexural modulus and Poisson's ratio effect the selection of an appropriate reinforced polymer for a chisel insert. Constraining a polymer insert created a hydrostatic compressive loading condition on the insert, thus increasing its apparent modulus of elasticity and improving its force transmission characteristics. While no significant increase in measured stiffness resulted from preloading of the chisel with a polymer insert prototype, hardening of the polymer from compressive impact loading was found to increase the durability of the exposed polymer insert material during actual tool operation.

The incorporation of a constrained polymer insert to chisel design prevents metal-to-metal impact between the piston and chisel components in power tool systems. Clearly, conventional chisel accessories produce high levels of sound that could damage the ear along with magnitudes and frequencies of vibration that contribute to biomechanical injuries over time. Prototype chisels have attenuated both sound and vibration emissions from the power tool system. While chisels with a polymer insert have survived over 1 hour of time in a running tool, more testing is needed to confirm the cutting effectiveness and durability of the new chisel systems.

Optimization of insert geometry for stiffness and durability will improve the transmission of impact energy. To further evaluate force transmission characteristics, finite element modeling should be completed for the conventional chisel as well as both constrained and unconstrained polymer inserts designs. Additionally, the relationship

51

between original protrusion length and desired preload applied to a prototype chisel prior to running in a tool should be investigated. The combination of these two variables and the correlation to prototype chisel durability and life has not been examined in enough detail to propose a final insert geometry and preloading specification at this time.

Finally, the constrained configuration of the insert within the chisel housing was proven to increase force transmission. The unique inverted conical frustum shape of the protruding polymer material resulting from the interference fit between the cylindrical insert and side chisel walls should be examined for similar performance advantages.

REFERENCES

[1] United States Department of Labor, Bureau of Labor Statistics, (2004). Table R27:

Detailed Source of Selected Events and Exposures. Available online:

http://www.bls.gov/iif/oshwc/osh/case/ostb1537.pdf (accessed April 2, 2006).

[2] United States Navy, Navy Safety Center. Acquisition Safety Vibration. Available

online: http://www.safetycenter.navy.mil/acquisition/vibration/default.htm

(accessed April 2, 2006).

[3] United States Department of Labor, Occupational Safety and Health Administration,

(2000). Ergonomics Rules: OSHA's Final Ergonomics Standard.

http://www.spineuniverse.com/displayarticle.php/article1405.html (accessed April

2, 2006).

[4] Glancey, J.L., J. Moore, D. Muhlenforth, J. Lawrence, (2004). Measurement of

Manual and Power Impact Tool Vibration Transmission to the Hand. Paper

No.047027. Written for Presentation at the 2004 ASAE/CSAE Annual

International Meeting, Ottawa, Ontario, Canada.

[5] Glancey, J.L., P. Popper (Dupont), T. Nasr, P. Truitt, M. Orgovan, D. O'Brian,

(2003). Design and Performance of Hand-Struck Impact Tools Using High

Performance Engineering Polymers. Paper No. IMECE2003-41455. Proceedings

of the 2003 ASME International Annual meeting, Washington, D.C.

[6] The Dupont Company, Plastics Homepage. Americas Data Sheets.

http://plastics.dupont.com/NASApp/myplastics/Mediator?id=0 (accessed January

4, 2006).

Appendix A

COMPLETE *MATLAB*™ CODE
NOTE: BOTH M-FILES MUST BE OPEN TO RUN SIMULATIONS

<u>M-FILE #1</u>

```
%2/1/06

function zprime=pneumdamp(t,z)

%dimensionless eq's
%pneum.m calc's derivatives displacements and velocitys (piston, chisel)
%nonlinear effects included
%prog start 1/4/05

global A;
y1=max(-A(7)*z(1),0);
y2=max(A(9)*(z(1)-z(2)-1),0);
ys=min(A(6)*z(2),A(1)+z(2));

%solve for yw; depends whether chisel cutting or retracting from "work"
if ((z(4))<0);
   yw=0;
else
   ((z(4))>0);
   yw=A(8)*z(2);
end

yp=A(2)*tanh(A(5)*(A(4)-z(1)));
%other alternative: yp=(A(2)/2)*tanh(A(5)*(A(4)-z(1)))+A(2)/2;

yd1=A(10)*z(3);
yd2=A(11)*z(4);
yf1=A(12);
yf2=A(13);
zprime=[z(3) z(4) (y1-y2+yp-yd1-yf1)/A(3) y2-yw-ys-yd2-yf2]';
```

M-FILE #2

```matlab
%PneumChisel2.m  simulation of pneumatic chisel prog start 1/4/05

%5/10/06 version

clear all

%INPUTS
Linsert=0.6;        %units (in)
Lchisel=9.765;      %measured=6.765
Dinsert=0.283;      %(in)
Dchisel=0.398;    %(in)
Areainsert=pi*Dinsert^2/4; %(in^2)
Areachisel=pi*Dchisel^2/4; %(in^2)
Fr=6.88;            %residual spring force (lb)

% step:  CHOOSE CORRECT MASS MODEL
%PISTON component mass is m1; CHISEL component mass is m2
%m1=81;     %measured mass piston with insert (g) ; bored piston=78.65
           %insert with L=0.56 inches has mass of 1.74
%m2=156;   %measured mass chisel without insert (g)
%masses for the CHISEL INSERT
m1=93;      % measured mass piston without insert (g)

%CALCULATE THE CHISEL MASS
%m2=151.36;              %mass chisel with insert (g) --> measured value
densitysteel=0.2836;     %units: lb/cu. in ; plain mild steel, 7.85 g/cu.cm
densitypolymer=0.053;  %units: lb/cu. in
%steel=0.2836 minlon=0.053 hytrel=0.0455
mchisel=densitysteel*Areachisel*Lchisel*454;
%if Lchisel=9.765in, mchisel=156.4193g
minsert=densitypolymer*Areainsert*Linsert*454;
%if Linsert=0.6in, minsert=0.9081g
m2=((densitysteel*Areachisel*Lchisel)-
(densitysteel*Areainsert*Linsert)+(densitypolymer*Areainsert*Linsert))*454
%units: (g)
%if no insert, m2=156.4
%if Lchisel=6.765in, m2=104.413g
%if Lchisel=9.765in, m2=152.4681g

%MORE INPUTS
Kr=140;     %retaining spring const (lb/in)
Dp=0.746;   %piston dia (in)
Lp=1.81;    %piston length (in)
L=2.345;    %stroke (in)
```

```matlab
p=90;        %pressure (psi)
Area=pi*Dp^2/4;
Fdim=Kr*L;
tau=sqrt((m2/(454*32.2))/(12*Kr));
xdim=Fdim/Kr;

%DIMENSIONLESS INPUTS
alpha=Fr/(Kr*L);    %A(1) resid force in retaining spring
beta=p*Area/(Kr*L); %A(2) press force/delta spring force with L displ
gamma=m1/m2;        %A(3) piston insert: mass piston/mass chisel
delta=.6;           %A(4) pressure reversal point/stroke length
xi=100;             %A(5) sharpness parameter for pressure reversal

%SOLVE FOR CONSTANT Kp:
% steps:  1) set correct Einsert
%         2) set correct v
Esteel=30015000;
%APPROXIMATION MODEL - axially loaded beam: AE/L
Einsert=760000;
%in psi: minlon=760,000 hytrel=82,650
%IDEAL MODEL - confined insert with effective stiffness E'
v=0.4;
%steel=0.28 minlon=0.4 hytrel=0.45
Eprime=((Einsert*(v-1))/(2*v^2+v-1))
%in psi: steel=N/A minlon=1,628,600 hytrel=313,500

Ki=(Areainsert*Einsert)/Linsert;
Kiconfined=(Areainsert*Eprime)/Linsert
Kc=(Areachisel*Esteel)/Lchisel;
Kpiston=(Area*Esteel)/Lp;
Kp=(Ki*Kpiston)/(Ki+Kpiston);
%for piston insert Kp=(Ki*Kc)/(Ki+Kc);
Kpconfined=(Kiconfined*Kpiston)/(Kiconfined+Kpiston);
%for piston insert change Kpiston to Kc
%for unmodified tool - model is solid piston impacting solid chisel
Kpnoinsert=(Kpiston*Kc)/(Kpiston+Kc);
jpcalc=Kp/Kr;  %approx
jpconfinedcalc=Kpconfined/Kr;  %ideal
jpnoinsertcalc=Kpnoinsert/Kr;   %ideal

%PARAMETER VALUES
% step:  substitute correct Jp value below
jstop=10000;       %A(6) stiffness of chisel "stop"/spring stiffness
jb=1000;           %A(7) stiffness of back polymer/spring stiffness
jw=3571;           %A(8) effective stiffness "work"/spring stiffness
Kw=500000;          %500000 from past Glancey journal article
```

```matlab
%Kw=500;          %low Kw approximates tool cutting air
jp=jpconfinedcalc;  %A(9) stiffness of chisel and polymer tip/spring stiffness
%for APPROXIMATION: steel=15672 minlon11C40=563 hytrel7246=62
%for IDEAL: no insert=2595 minlon11C40=1192 hytrel7246=234

%BUILD IN FRICTION TO THE MODEL
damp1=0;          %A(10) damper piston/spring damper
damp2=0;          %A(11) damper chisel/spring damper
fr1=0;            %A(12) coulomb friction piston/spring stiffness
fr2=0;            %A(13) coulomb friction chisel/spring stiffness

A=[alpha beta gamma delta xi jstop jb jw jp damp1 damp2 fr1 fr2]';
global A;

%x1 = displ of pistion (from just touching back spring
%x2 = displ of chisel (from just touching "stop"
%y1 = dim'less force on back of pistion
%y2 = dim'less force on front of pistion
%yw = dim'less force on work
%yp = dim'less net pressure force on back of pistion
%yd1 = dim'less damping on piston
%yd2 = dim'less damping on chisel
%yf1 = dim'less coulomb friction on piston
%yf2 = dim'less coulomb friction on chisel

%COMPUTATION PARAMETERS
DeltaT=8;          %total time in calc (d'mless time)
%FOR MULTIPLE IMPACTS: make DeltaT larger!
tspan=[0 DeltaT]; %range of calc
z0=[0;0;0;0];      %initial conditions for diff eq

%FIND SOLUTION OF DIFFERENTIAL EQUATION
[t,z]=ode45('pneumdamp',tspan,z0);  %NON-STIFF INTEGRATOR
%z(:,1) is displacement of mass1
%z(:,2) is displacement of mass2
%z(:,3) is velocity of mass1
%z(:,4) is velocity of mass2

%CONVERT BACK TO MEANINGFUL UNITS
tsec=t*tau;
x1inch=z(:,1)*xdim;
realxpiston=max(x1inch);
x2inch=z(:,2)*xdim;
realxchisel=max(x2inch);
x3inpersec=(z(:,3)*xdim)/tau;
velpiston=max(x3inpersec);
```

```matlab
x4inpersec=(z(:,4)*xdim)/tau;

%FIND THE MAXIMUM FORCE AT BOTTOM (OUTPUT FORCE) OF CHISEL
dimout=Kw*z(:,2);
output=Kw*x2inch;
maxbottomforce=max(output)

%CALCULATE/ALTER LENGTHS OF VECTORS TO MATCH FOR GRAPHS
timespan=[t*tau];
length(timespan);
len=length(timespan);
newlen=len-1;
minusonetime=timespan(1:newlen);
length(output);
leno=length(output);
newleno=leno-1;
minusoneoutput=output(1:newleno);
length(minusoneoutput);

%SOLVE FOR dt
deltat=diff(timespan);

%SOLVE FOR dv
deltav2=diff(z(:,4));

%SOLVE FOR THE ACCEL OF CHISEL
v2dot=deltav2./deltat;

%FIND THE MAXIMUM FORCE AT THE TOP OF CHISEL
top=(minusoneoutput+((m2/(454*32.2))*v2dot));
maxtopforce=max(top)

%CONVERT RESULTS TO METRIC UNITS
mx1=x1inch*2.54; %units: cm
mx2=x2inch*2.54; %units: cm
mx3=x3inpersec*0.0254; %units: m/sec
mx4=x4inpersec*0.0254; %units: m/sec
mv2dot=v2dot*0.0254; %units: m/sec^2
mtop=top*4.44822162; %units: N
moutput=output*4.44822162; %units: N
kntop=mtop/1000; %units: kN
knoutput=moutput/1000; %units: kN

mmaxtopforce=max(mtop); %units: kN
mmaxoutput=max(moutput); %units: kN
mmaxkntop=max(kntop) %units: kN
```
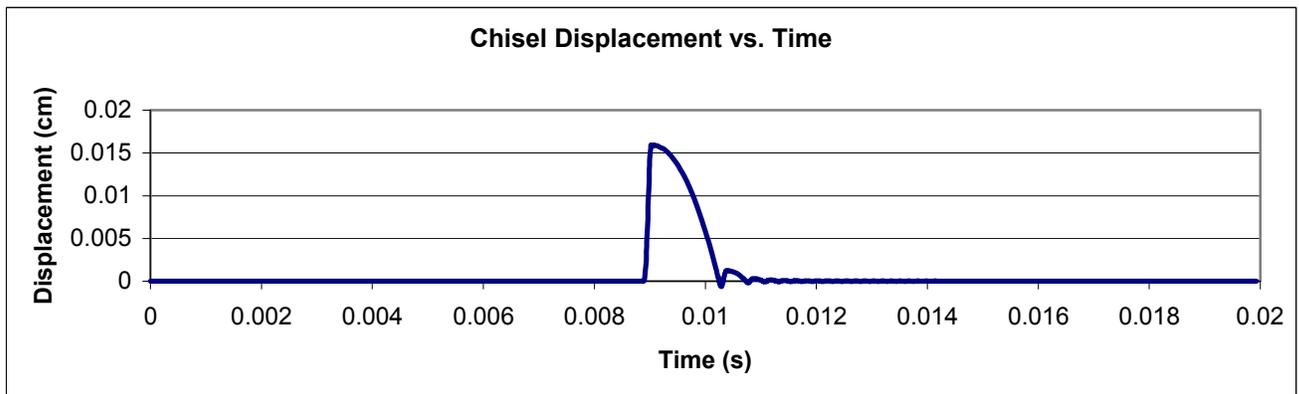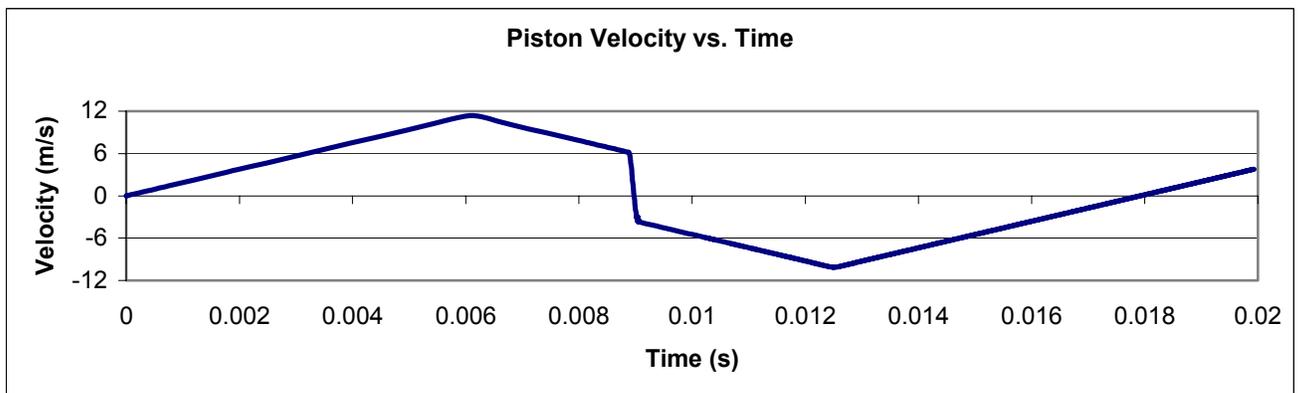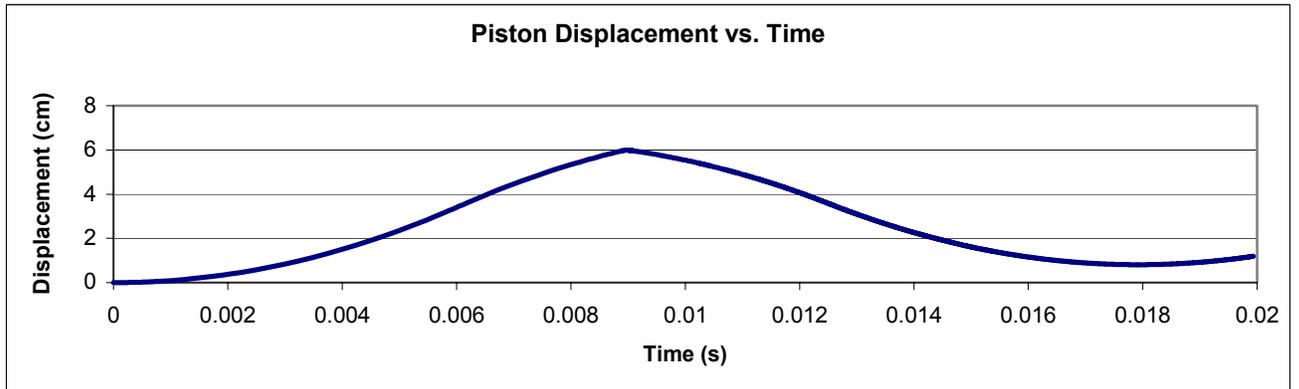
```matlab
mmaxknoutput=max(knoutput) %units: kN

%RESULTS PLOTTED
subplot(7,1,1)
plot(tsec,x1inch)
title('PISTON DISPLACEMENT')
xlabel('time (sec)')
ylabel('displacement (in)')
subplot(7,1,2)
plot(tsec,x2inch)
title('CHISEL DISPLACEMENT')
xlabel('time (sec)')
ylabel('displacement (in)')
subplot(7,1,3)
plot(tsec,x3inpersec)
title('PISTON VELOCITY')
xlabel('time (sec)')
ylabel('velocity (in/sec)')
subplot(7,1,4)
plot(tsec,x4inpersec)
title('CHISEL VELOCITY')
xlabel('time (sec)')
ylabel('velocity (in/sec)')
subplot(7,1,5)
plot(minusonetime,v2dot)
title('CHISEL ACCELERATION')
xlabel('time (sec)')
ylabel('accel (in/sec)')
subplot(7,1,6)
plot(minusonetime,top)
title('TOP OF CHISEL FORCE')
xlabel('time (sec)')
ylabel('Ftop (lbf)')
subplot(7,1,7)
plot(tsec,output)
title('BOTTOM OF CHISEL FORCE')
xlabel('time (sec)')
ylabel('Fout (lbf)')
```
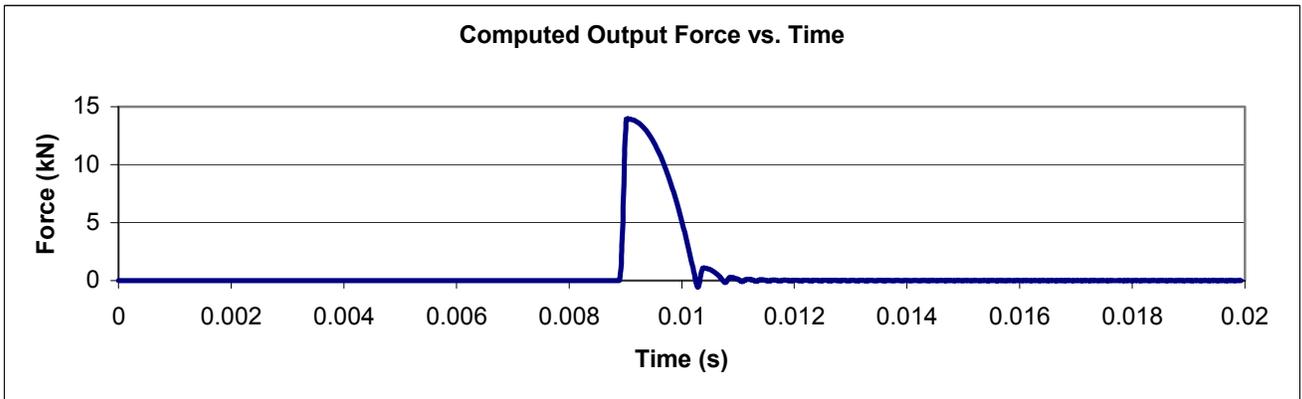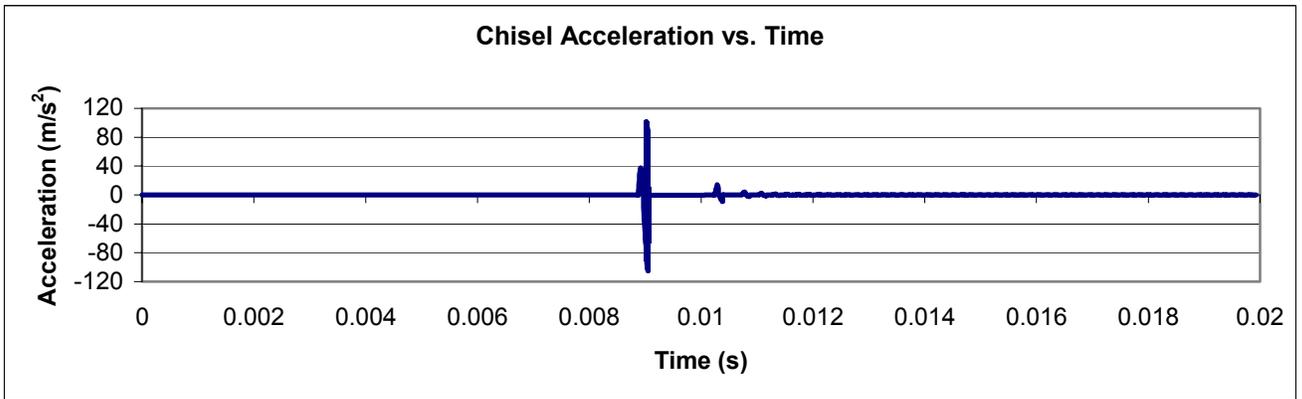
Appendix B

COMPLETE SIMULATION OUTPUTS FOR A PROTOTYPE CHISEL
(for the insert geometry: L = 1.5 cm, dia = 0.72 cm)

Piston Displacement vs. Time

Piston Velocity vs. Time

Chisel Displacement vs. Time

Chisel Velocity vs. Time

Chisel Acceleration vs. Time

Computed Output Force vs. Time
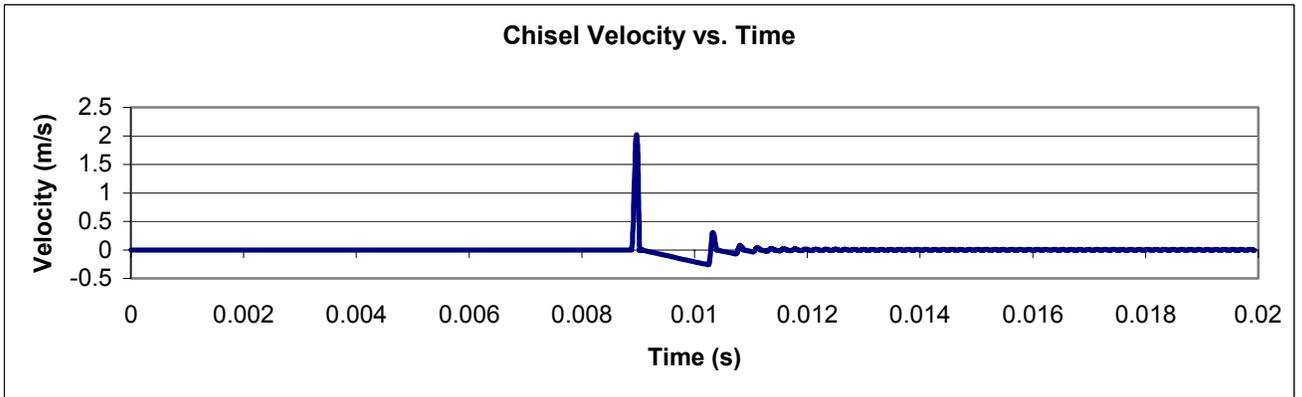
Appendix C

OUTPUT FORCE PREDICTION: CONSERVATION OF ENERGY
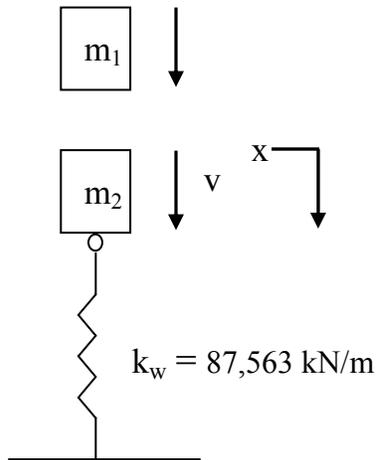
$$\frac{1}{2}m_1v^2 = \frac{1}{2}k_wx^2$$

$$\Rightarrow x = \left[\frac{m_1v^2}{k_w}\right]^{1/2}$$

$$F = k_wx = k_w\left[\frac{m_1v}{k_w}\right] = \sqrt{k_wm_1v^2}$$

$m_1 \downarrow$

$m_2 \downarrow v$ x

$k_w = 87{,}563 \text{ kN/m}$

where, $m_1 = 93$ grams and $v = \dfrac{\Delta s}{\Delta t} = \dfrac{5.96}{0.018}$ cm/s = 3.31 m/s

Therefore, $F = \sqrt{87{,}563{,}000}\sqrt{0.093 \times 3.31 \times 3.31}$

= 9445 N

= 9.45 kN

OUTPUT FORCE PREDICTION: THE IMPULSE-MOMENTUM THEOREM

Piston Velocity vs. Time

impact occurs
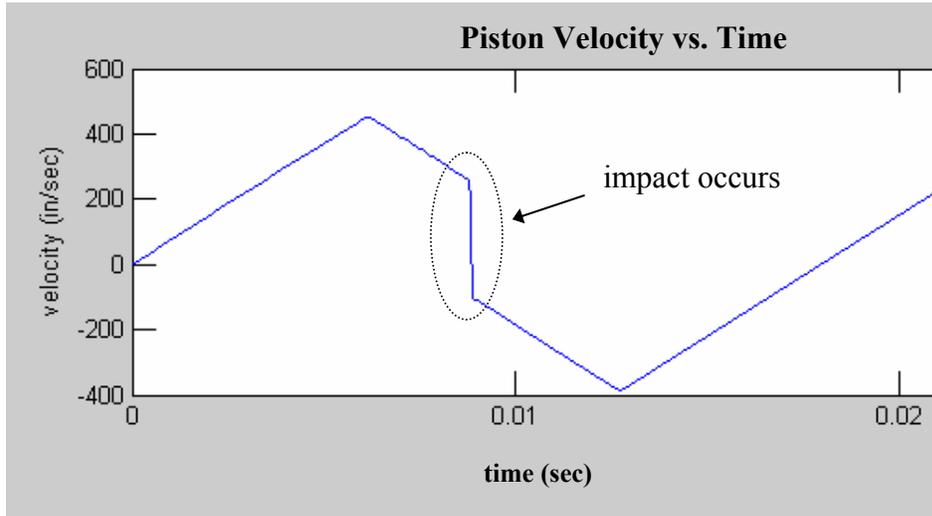
Zoom in on the impact zone:

Piston Velocity

8.92
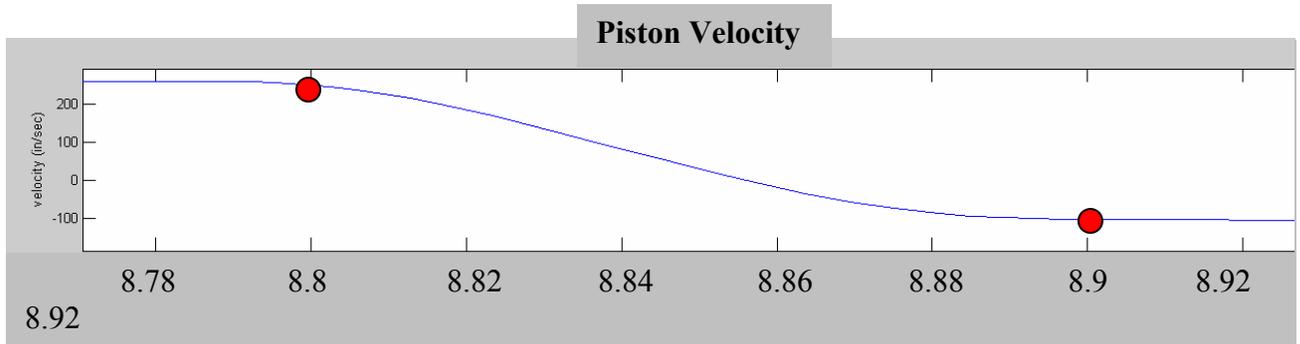
From graphical estimations:

Δt = 8.90 msec – 8.8 msec = 0.10 msec

Δv = 260 in/sec – (-110 in/sec) = 370 in/sec = 9.40 m/sec

Note: mass of piston = 93 grams

$$F\Delta t = m\Delta v$$

$$\Rightarrow F = m\frac{\Delta v}{\Delta t} = \frac{0.093 \text{ kg x } 9.40 \text{ m/sec}}{0.00010 \text{ sec}} = 8742 \text{ N} = 8.74 \text{ kN}$$

Appendix E

CAD DRAWING FOR A DUPLICATE PISTON COMPONENT

Ø0.412

Ø0.691

1.810

1.613

1.279

Ø0.703

0.044

$Ø0.746^{+0.000}_{-0.002}$

TOLERENCES (UNLESS OTHERVISE NOTED)

PROJECT OR CLASS: S&E RESEARCH

DECIMAL
.XXX ± .005
.XX ± .010
.X ± .050

DRAWING TITLE: PISTON-unmodified

DRAWN BY: Janelle Konchar DATE: 7/1/2004

FRACTIONAL ± 1/32

APPROVED BY: DATE:

MATERIAL: steel QUANITY: 1

ANGULAR ± 0.5 DEG

SCALE: 2:1 DRG NO:

BILLING ACCOUNT:

NOTE: break all corners
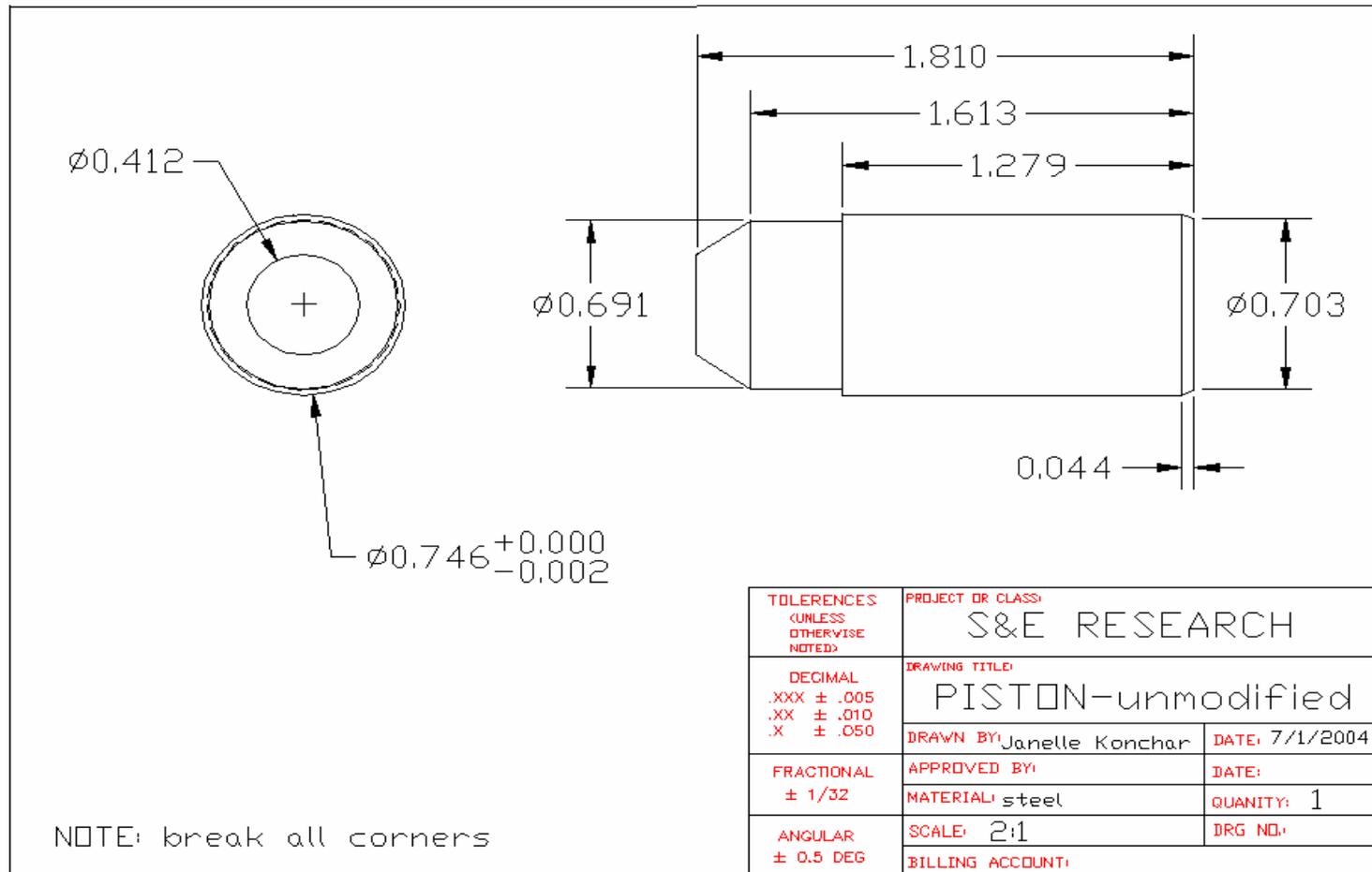
CAD DRAWING FOR A PISTON WITH A FRONT POLYMER INSERT

Ø0.412

Ø0.746 +0.000 −0.002

Ø0.4062 +0.0000 −0.0005

1.810

0.531

0.531

0.197

0.044

Ø0.691

Ø0.703

35°

26°

NOTE: break all corners

TOLERENCES (UNLESS OTHERVISE NOTED)	PROJECT OR CLASS S&E RESEARCH	
DECIMAL .XXX ± .005 .XX ± .010 .X ± .050	DRAWING TITLE PISTON – front Insert	
	DRAWN BY Janelle Konchar	DATE 11/5/2004
FRACTIONAL ± 1/32	APPROVED BY	DATE 1
	MATERIAL steel	QUANITY:
ANGULAR ± 0.5 DEG	SCALE 2:1	DRG NO:
	BILLING ACCOUNT:	

Appendix G

CAD DRAWING FOR A PROTOTYPE CHISEL

TOLERENCES (UNLESS OTHERWISE NOTED)	PROJECT OR CLASS: Chisel Prototype	
	DRAWING TITLE: Drilled Out Chisel	
DECIMAL .XXX ± .005 .XX ± .010 .X ± .050	DRAWN BY: J. Glancey	DATE:
	APPROVED BY:	DATE:
FRACTIONAL ± 1/32	MATERIAL:	QUANITY:
ANGULAR ± 0.5 DEG	SCALE:	DRG NO.:
	BILLING ACCOUNT:	

Appendix H

CAD DRAWING FOR A POLYMER CHISEL INSERT
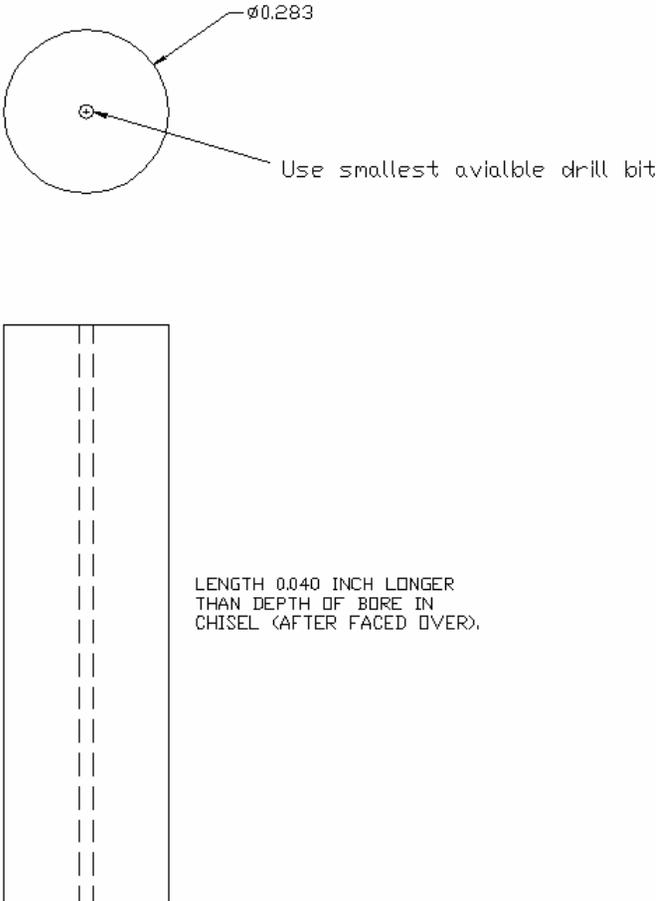
Ø0.283

Use smallest avialble drill bit.

Notes:
Drawn for 0.005 Inch Interference fit.
Face off tool before inserting polymer insert.
Dimensions in inches.
Break sharp edges.

LENGTH 0.040 INCH LONGER
THAN DEPTH OF BORE IN
CHISEL (AFTER FACED OVER).

TOLERENCES (UNLESS OTHERWISE NOTED)	PROJECT OR CLASS: HardCap Air Hammer Project	
DECIMAL .XXX ± .005 .XX ± .010 .X ± .050	DRAWING TITLE: Air Hammer Tool Insert	
	DRAWN BY: Matthew Griffith	DATE: 01/04/06
FRACTIONAL ± 1/32	APPROVED BY:	DATE:
	MATERIAL: Minlon 11C40	QUANITY:
ANGULAR ± 0.5 DEG	SCALE: 4:1	DRG NO:
	BILLING ACCOUNT:	

68

Appendix I

CAD DRAWING FOR THE CHISEL TEST FIXTURE